



Naturalis Repository

## Paleoenvironmental inferences on the Late Miocene hominoid-bearing site of Can Llobateres

Sara G. Arranz, Isaac Casanovas-Vilar, Indrė Žliobaitė, Juan Abella, Chiara Angelone, Beatriz Azanza, Raymond Bernor, Omar Cirilli, Daniel DeMiguel, Marc Furió, Luca Pandolfi, Josep M. Robles, Israel M. Sánchez, Lars W. van den Hoek Ostende, David M. Alba

### DOI

<https://doi.org/10.1016/j.jhevol.2023.103441>

### Downloaded from

[Naturalis Repository](#)

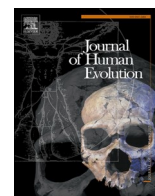
### Article 25fa Dutch Copyright Act (DCA) - End User Rights

This publication is distributed under the terms of Article 25fa of the Dutch Copyright Act (Auteurswet) with consent from the author. Dutch law entitles the maker of a short scientific work funded either wholly or partially by Dutch public funds to make that work publicly available following a reasonable period after the work was first published, provided that reference is made to the source of the first publication of the work.

This publication is distributed under the Naturalis Biodiversity Center 'Taverne implementation' programme. In this programme, research output of Naturalis researchers and collection managers that complies with the legal requirements of Article 25fa of the Dutch Copyright Act is distributed online and free of barriers in the Naturalis institutional repository. Research output is distributed six months after its first online publication in the original published version and with proper attribution to the source of the original publication.

You are permitted to download and use the publication for personal purposes. All rights remain with the author(s) and copyrights owner(s) of this work. Any use of the publication other than authorized under this license or copyright law is prohibited.

If you believe that digital publication of certain material infringes any of your rights or (privacy) interests, please let the department of Collection Information know, stating your reasons. In case of a legitimate complaint, Collection Information will make the material inaccessible. Please contact us through email: [collectie.informatie@naturalis.nl](mailto:collectie.informatie@naturalis.nl). We will contact you as soon as possible.



## Paleoenvironmental inferences on the Late Miocene hominoid-bearing site of Can Llobateres (NE Iberian Peninsula): An ecometric approach based on functional dental traits

Sara G. Arranz<sup>a,\*</sup>, Isaac Casanovas-Vilar<sup>a</sup>, Indrė Žliobaitė<sup>b,c</sup>, Juan Abella<sup>d,a,e</sup>, Chiara Angelone<sup>f,g</sup>, Beatriz Azanza<sup>h</sup>, Raymond Bernor<sup>i,j</sup>, Omar Cirilli<sup>i,k</sup>, Daniel DeMiguel<sup>h,l,a</sup>, Marc Furió<sup>m,a</sup>, Luca Pandolfi<sup>n</sup>, Josep M. Robles<sup>a</sup>, Israel M. Sánchez<sup>a</sup>, Lars W. van den Hoek Ostende<sup>o</sup>, David M. Alba<sup>a,\*</sup>

<sup>a</sup> Institut Català de Paleontologia Miquel Crusafont, Universitat Autònoma de Barcelona, c/ Columnes s/n, 08193 Cerdanyola del Vallès, Barcelona, Spain

<sup>b</sup> Department of Computer Science, University of Helsinki, P.O. Box 68, 00014 Helsinki, Finland

<sup>c</sup> Department of Geosciences and Geography, University of Helsinki, P.O. Box 64, 00014 Helsinki, Finland

<sup>d</sup> Grup d'Investigació en Paleontologia de Vertebrats del Cenozoic (PVC-GIUV), Departament de Botànica i Geologia, Universitat de València, 46100 Burjassot, València, Spain

<sup>e</sup> Instituto Nacional de Biodiversidad (INABIO), Pje. Rumipamba N. 341 y Av. de los Shyris (Parque La Carolina), Quito, Ecuador

<sup>f</sup> Dipartimento di Scienze, Università degli Studi Roma Tre, 00146 Roma, Italy

<sup>g</sup> Key Laboratory of Vertebrate Evolution and Human Origins, Institute of Vertebrate Paleontology and Paleoanthropology, Chinese Academy of Sciences, 100044 Beijing, China

<sup>h</sup> Departamento de Ciencias de la Tierra, and Instituto Universitario de Investigación en Ciencias Ambientales de Aragón (IUCA), Universidad de Zaragoza, 50009, Zaragoza, Spain

<sup>i</sup> College of Medicine, Department of Anatomy, Laboratory of Evolutionary Biology, Howard University, 520 W St. N.W., 20059, Washington D.C., USA

<sup>j</sup> Human Origins Program, Department of Anthropology, National Museum of Natural History, Smithsonian Institution, 20013, Washington D.C., USA

<sup>k</sup> Department of Paleobiology, National Museum of Natural History, Smithsonian Institution, MRC 121, 20013, Washington, D.C., USA

<sup>l</sup> ARAID Foundation, 50018, Zaragoza, Spain

<sup>m</sup> Serra Hünter Fellow, Departament de Geologia, Universitat Autònoma de Barcelona, Campus de la UAB, 08193 Cerdanyola del Vallès, Barcelona, Spain

<sup>n</sup> Dipartimento di Scienze, Università della Basilicata, Via dell'Ateneo Lucano, 10, 85100, Potenza, Italy

<sup>o</sup> Naturalis Biodiversity Center, Darwinweg 2, 2333 CR Leiden, the Netherlands

### ARTICLE INFO

#### Keywords:

Fossil apes  
*Hispanopithecus*  
 Functional crown types  
 Paleocology  
 Vallesian  
 Spain

### ABSTRACT

*Hispanopithecus laietanus* from the Late Miocene (9.8 Ma) of Can Llobateres 1 (CLL1; Vallès-Penedès Basin, NE Iberian Peninsula) represents one of the latest occurrences of fossil apes in Western mainland Europe, where they are last recorded at ~9.5 Ma. The paleoenvironment of CLL1 is thus relevant for understanding the extinction of European hominoids. To refine paleoenvironmental inferences for CLL1, we apply ecometric models based on functional crown type (FCT) variables—a scoring scheme devised to capture macroscopic functional traits of occlusal shape and wear surfaces of herbivorous large mammal molars. Paleotemperature and paleoprecipitation estimates for CLL1 are provided based on published regional regression models linking average FCT of large herbivorous mammal communities to climatic conditions. A mapping to Whittaker's present-day biome classification is also attempted based on these estimates, as well as a case-based reasoning via canonical variate analysis of FCT variables from five relevant biomes. Estimates of mean annual temperature (25 °C) and mean annual precipitation (881 mm) classify CLL1 as a tropical seasonal forest/savanna, only in partial agreement with the canonical variate analysis results, which classify CLL1 as a tropical rainforest with a higher probability. The former biome agrees better with previous inferences derived from fossil plants and mammals, as well as preliminary isotopic data. The misclassification of CLL1 as a tropical forest is attributed to the mixture of forest-adapted taxa with others adapted to more open environments, given that faunal and plant composition indicates the presence of a dense wetland/riparian forest with more open woodlands nearby. The tested FCT ecometric approaches do not provide unambiguous biome classification for CLL1. Nevertheless, our results are

\* Corresponding authors.

E-mail addresses: [sara.arranz@icp.cat](mailto:sara.arranz@icp.cat) (S.G. Arranz), [david.alba@icp.cat](mailto:david.alba@icp.cat) (D.M. Alba).

<https://doi.org/10.1016/j.jhevol.2023.103441>

Received 1 February 2023; Accepted 15 September 2023

Available online 17 October 2023

0047-2484/© 2023 Elsevier Ltd. All rights reserved.

consistent with those from other approaches, thus suggesting that FCT variables are potentially useful to investigate paleoenvironmental changes through time and space—including those that led to the extinction of European Miocene apes.

## 1. Introduction

### 1.1. The hominoid-bearing site of Can Llobateres

**Historical background** The fossil site of Can Llobateres (Late Miocene), in the municipality of Sabadell (Catalonia, NE Spain), has figured prominently in the study of Miocene mammals from Europe—being considered the reference locality of MN9 (Mein, 1990)—with emphasis on fossil hominoids. The site was discovered in 1926 (Crusafont Pairó, 1969; Alba et al., 2011a, 2011b), and the first accounts of its fauna were published in the 1940s (Villalta Comella and Crusafont Pairó, 1943; Crusafont Pairó and Villalta Comella, 1948). Hominoid dental remains, assigned to the dryopithecine<sup>1</sup> *Hispanopithecus laietanus*, were first discovered there in 1958 (Crusafont Pairó, 1958; Crusafont Pairó and Hürzeler, 1969), and additional hominoid remains were subsequently recovered during the 1960s (Crusafont Pairó and Hürzeler, 1961, 1969; Crusafont Pairó, 1965; Golpe Posse, 1982, 1993; Moyà-Solà et al., 1990). Crusafont and Hürzeler (1961, 1969) reported two additional species from the site—never figured or described, and hence considered nomina nuda (Szalay and Delson, 1979; Alba, 2012; Alba et al., 2012a)—while a fourth hominoid was subsequently reported based on an isolated male upper canine (Crusafont Pairó and Golpe Posse, 1973), being attributed to *Sivapithecus indicus*.

In 1981, additional dental hominoid material was recovered from the lower levels of the site (Begun et al., 1990; Golpe Posse, 1993), known as Can Llobateres 1 (CLL1). From 1992 onward, a partial cranium (Moyà-Solà and Köhler, 1993, 1995; Begun, 1994) and skeleton (Moyà-Solà and Köhler, 1996; Almécija et al., 2007; Pina et al., 2012; Tallman et al., 2013; Susanna et al., 2014) were discovered on the upper levels of the site, termed Can Llobateres 2 (CLL2), which were last excavated in 1997. In 2010, excavations were resumed again at CLL1 by a team led from the Institut Català de Paleontologia Miquel Crusafont (ICP), and additional hominoid teeth were found (Alba et al., 2012a), along with plant remains that enabled a better characterization of the paleoenvironment (Marmi et al., 2012). The locality of CLL1 was last excavated in 2015, owing to the paucity of the fossiliferous levels that delivered most of the hominoid dental remains in previous years. Begun et al. (1990) and most subsequent authors attributed the whole hominoid sample from Can Llobateres to *Dryopithecus laietanus* (Harrison, 1991; Moyà-Solà and Köhler, 1993, 1995, 1996; Begun, 1994; Ribot et al., 1996) or, more recently, *H. laietanus* (Cameron, 1997, 1998, 1999, 2004; Almécija et al., 2007; Moyà-Solà et al., 2009; Begun, 2009; Alba, 2012; Alba et al., 2012a).

**Geological background and taphonomical remarks** Can Llobateres is located in the Vallès sector of the Vallès-Penedès Basin (Catalonia, Spain; Fig. 1), an elongated half-graben about 100 km in length and 12–14 km in width, parallel to the Catalan coastline near Barcelona, and bounded by the Catalan Coastal Ranges (for an updated review, see Casanovas-Vilar et al., 2016a). The Miocene sedimentary infill of the Vallès-Penedès Basin has been divided into four main lithostratigraphic units, Can Llobateres belonging to the Upper Continental Units, which range from the Middle to the Late Miocene (Casanovas-Vilar et al., 2016a). In particular, Can Llobateres is located within distal facies of the

alluvial fan system of Castellar del Vallès (Agustí et al., 1996, 1997), consisting of a short (~20 m-thick) sequence, mostly defined by mudstones (claystones and siltstones), as well as polymictic breccias and conglomerates (Marmi et al., 2012; Alba et al., 2012a). The locality of CLL1 is located in the lower section of the sequence, characterized by organic matter and abundant mudstones, indicating a poorly drained alluvial plain that would have favored the development of small shallow lakes and ponds (Agustí et al., 1996; Alba et al., 2011a, 2011b, 2012a).

No taphonomic study has been performed at CLL1, but Begun et al. (1990) made some sedimentological and taphonomic remarks based on the 1981 campaign, while Marmi et al. (2012) and Alba et al. (2012a) provided far more detailed sedimentological descriptions and additional taphonomic details based on the 2010–2011 campaigns. The former authors distinguished two ‘sedimentary units’ at CLL1, which they interpreted as corresponding to two different ‘fluvial cycles’ (Begun et al., 1990): the lower one, characterized by finer sediments indicative of a low-energy depositional environment, would have yielded taxa associated with humid and forested environments (such as primates and suids); the upper one, in turn, would be characterized by coarser sediments (including channel deposits) indicative of a higher-energy depositional environment and, according to these authors, would have yielded taxa indicative of more open conditions (such as hipparionin equids) that could have been transported from greater distances. Subsequent fieldwork at the site (Alba et al., 2012a) confirmed that primates are apparently restricted to the lower ‘unit’ recognized by Begun et al. (1990) but evinced a greater stratigraphic and taphonomic complexity (Marmi et al., 2012; Alba et al., 2012a), in which four stratigraphic bodies may be discerned.

The bottom of the CLL1 sequence (not available to Begun et al., 1990) is composed by layers of reddish to brown silts, sands, and conglomerates, indicative of less humid conditions than the ‘classical’ layers of CLL1, probably representing the end of a preceding depositional cycle (Alba et al., 2012a). The lower ‘unit’ of Begun et al. (1990), in turn, comprises variously colored mudstones (mostly fine-grained clays) with abundant micromammal and some macromammal remains (including the hominoid teeth recovered in 1981 and 2011), plus mollusk shells, silicified figs, and other fragmentary and poorly preserved plant remains. The lower layers (1a and 1b) are blackish and become lighter in color (light gray to greenish) toward the top (layer 2), although at different locations, layers 1b and 2—the ones that yielded primate remains—are completely light brown (Marmi et al., 2012; Alba et al., 2012a). The top layers (3a and 3b) consist of greenish to yellowish clays with some coarser sediments, in which gastropod shells are poorly preserved and vertebrate remains sparser than in the underlying layers. The upper ‘unit’ of Begun et al. (1990) begins with a paleochannel (layer 4a) of varying thickness composed of much coarser sediments (with decreasing granulometry from bottom to top), which at some point erodes some or all of the aforementioned layers and which locally yielded more abundant large mammal remains. Overlying these channel deposits, there is a thick (>2.5 m) sedimentary package (layer 4b/4p) of alternating green clays, greenish to orange silts, and conglomerates, which locally preserve abundant plant macroremains (Marmi et al., 2012). A fourth sedimentary body can be distinguished at the top of the CLL1 sequence, including a paleochannel (layer 5a) that erodes layer 4b and an overlying 6.5 m-thick package (layer 5b) of multiple episodes of ocher to red clays, silts, and conglomerates, indicative of paleosol formation and well-aerated conditions (Marmi et al., 2012).

Pending more detailed analyses, and contrary to Begun et al.’s (1990) previous assessment, the 2010–2015 fieldwork campaigns (D.M. A., pers. obs.) failed to confirm differences in faunal composition

<sup>1</sup> Although it is currently uncertain whether the Dryopithecinae constitute a clade or a paraphyletic assemblage (Alba, 2012; Almécija et al., 2021; Pugh, 2022), we follow Urciuoli and Alba (2023) in provisionally distinguishing this group at the subfamily rank until its phylogenetic relationships are clarified further.

between the primate-bearing layers and the paleochannel deposits (other than the apparent lack of primates in the latter). For example, suids are not restricted to the primate-bearing layers (contra Begun et al., 1990) but are also present in the paleochannel deposits (layer 4a) and in the layer 4b that overlies them. Similarly, *Hippotherium* remains are more abundant in layer 4a but are also present in most of the remaining layers, both above (4b) and below (3b, 2, and 1b), thus including the primate-bearing ones. Finally, the fact that forest-adapted taxa are not restricted to the latter is best exemplified by the recovery of a *Tapirus* tooth from the bottom of layer 4a (D.M.A., pers. obs.). Coupled with the fact that detailed stratigraphic provenance is not recorded for most of the remains recovered before 2010, this makes impossible to conclusively ascertain whether, in fact, CLL1 as a whole mixes faunal elements from different environments due to differential transport among various fossiliferous layers.

On the other hand, different degrees of transport depending on the layer are confirmed by available data. In particular, the presence of

isolated teeth from two single individuals (hominoid and cervid) scattered over a few square meters in one of the clay layers that yielded primate remains suggests minimal transport, probably under water (Alba et al., 2012a). By contrast, the paleochannel combines fragmentary and rounded remains of multiple large mammals with better-preserved and larger macromammal remains (including disarticulated dentognathic and postcranial remains of a single *Hippotherium* individual; D.M.A., pers. obs.)—overall indicative of transport in higher-energy conditions from longer distances than in the primate-bearing layers as previously concluded by Begun et al. (1990). Finally, the plant remains from layer 4p (Marmi et al., 2012) are interpreted as a parautochthonous assemblage accumulated by wind and short water transport in a shallow-water depositional environment. All this preliminary taphonomic evidence combined suggests that the fossil assemblages from CLL1 are representative of the fauna and flora present at and near the depositional environment, although it cannot be discounted that some taxa preferentially inhabited areas farther away from

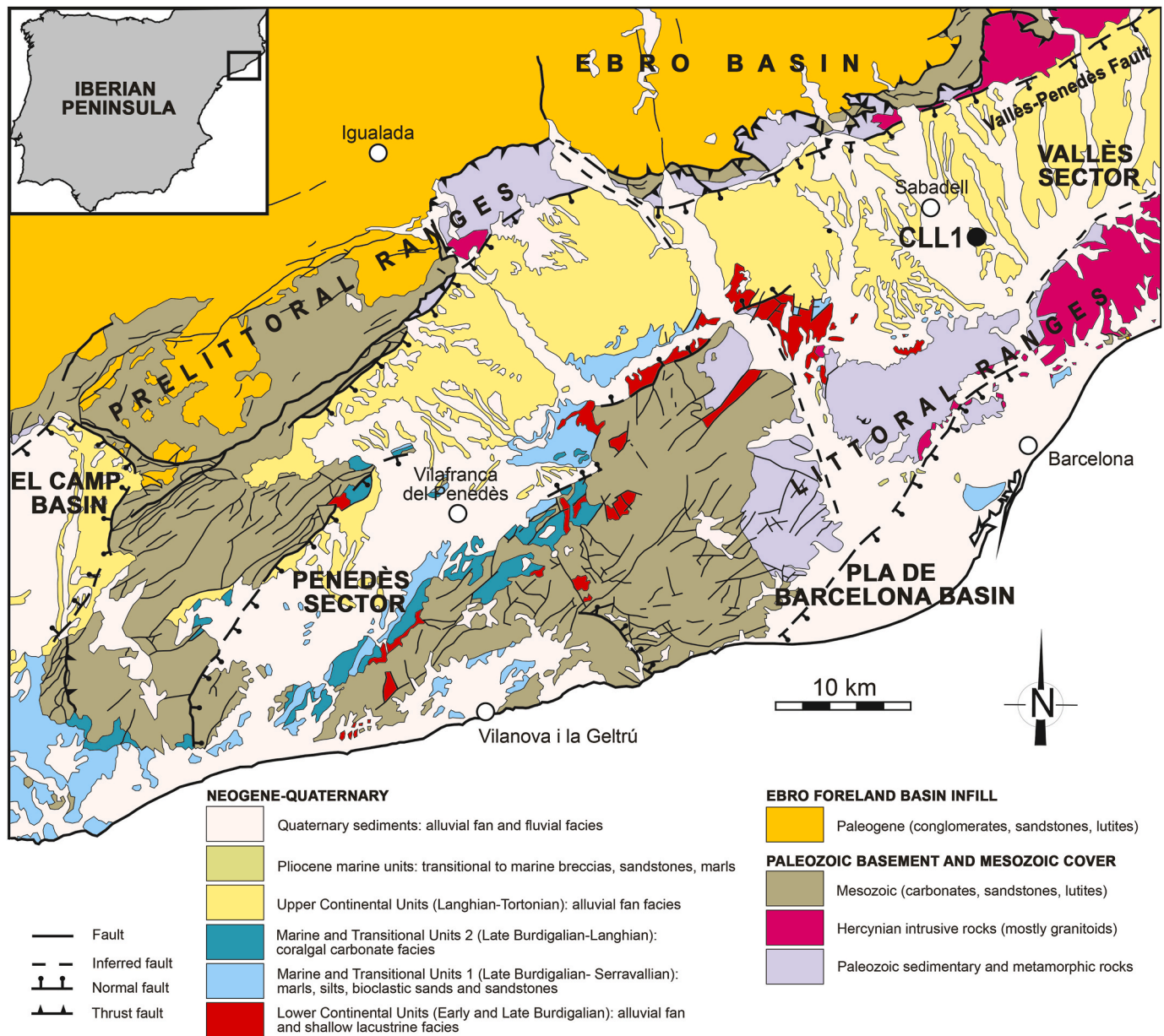


**Figure 1.** Simplified geological map of the Vallès-Penedès Basin showing the location of Can Llobateres 1 (CLL1) and location of the basin within the Iberian Peninsula (inset). Modified from Casanovas-Vilar et al. (2016a: Fig. 1). (For interpretation of the references to color in this figure legend, the reader is referred to the Web version of this article.)

it, as some fossiliferous layers evince greater degrees of transport than others.

**Chronological and paleoenvironmental background** On biostratigraphic grounds, CLL1 is correlated to the *Cricetulodon hartenbergeri-Progonomys hispanicus* interval local subzone, whereas CLL2 is correlated to the *Cricetulodon sabadellensis + Progonomys hispanicus* concurrent range local subzone (Casanovas-Vilar et al., 2016b). In addition, the Can Llobateres sequence records three magnetozones, with reverse polarity in the lower and upper parts and normal polarity in the middle (Agustí et al., 1996, 1997). In particular, CLL1 is correlated to C4Ar.3r, whereas CLL2 is correlated to C4Ar.2r (Agustí et al., 1996, 1997), with interpolated ages of 9.76 and 9.62 Ma, respectively (Casanovas-Vilar et al., 2016b). Based on the absence of *Progonomys* from CLL1, it has traditionally been considered that the Can Llobateres sequence records the early to the late Vallesian transition, with CLL1 and CLL2 being correlated to MN9 and MN10, respectively (Agustí et al., 1996, 1997; Alba et al., 2012a); indeed, CLL1 is considered the reference locality for MN9 (Mein, 1990; de Bruijn et al., 1992; Casanovas-Vilar et al., 2016b). However, *Progonomys* remains have been found in older sites from other Iberian basins, placing the lower boundary of MN10 (as defined by the first common occurrence of this genus) at 9.98 Ma (Hilgen et al., 2012; Van Dam et al., 2014). Accordingly, under a strictly biostratigraphic approach to MN units, CLL1 must be correlated to MN10 instead of MN9 (Casanovas-Vilar et al., 2016b; Alba et al., 2018). It is unlikely that the paleobiodiversity of CLL1 is inflated by time averaging as most of the remains come from a short stratigraphic interval of ~2 m (Alba et al., 2012a). Based on the average sedimentation rate for the Vallesian of the Vallès-Penedès Basin (20 cm/kyr; Garcés et al., 1996), this would merely represent a time interval of ~10 kyr—in rough agreement with the difference between the interpolated ages of CLL1 and CLL2 (~140 kyr; Casanovas-Vilar et al., 2016b), which are separated by less than 20 m of stratigraphic distance.

Paleoenvironmental inferences have previously been drawn for CLL1 based on both mammals and plants, using different methods—see summary in Table 1 and the Discussion for additional details. The plant remains (Álvarez Ramis, 1975; Sanz de Siria Catalán, 1993, 1994; Alba et al., 2011b; Marmi et al., 2012), which enable a reliable reconstruction of the paleoenvironment that *H. laietanus* inhabited, are generally in agreement with the conclusions drawn from the large and/or small mammals (Nagatoshi, 1987; Köhler, 1993; Andrews, 1996; Hernández Fernández et al., 2003; Costeur, 2005; Casanovas-Vilar and Agustí, 2007), which indicate the presence of a humid and closed forest paleoenvironment at the depositional area but further hint at the existence of relatively more open woodlands nearby (Marmi et al., 2012). Some paleoenvironmental conclusions have also been derived for CLL1 from the numerical analyses of its mammalian assemblage composition (Andrews, 1996; Hernández Fernández et al., 2003), and ecometrics in general have been applied to this site as part of studies that aimed to reconstruct continental patterns of Neogene paleoprecipitation (Fortelius et al., 2002; Eronen et al., 2009, 2010a; Kaya et al., 2018) or net

primary production (Toivonen et al., 2022). However, no dedicated ecometric approaches to paleoenvironment reconstruction have been performed thus far. Given that *H. laietanus* is the latest hominoid recorded from mainland Western Europe, the reconstruction of its paleoenvironment is highly significant for understanding the local extinction of hominoids and other mammalian taxa in Europe during the Late Miocene (Casanovas-Vilar et al., 2011).

## 1.2. Ecometrics and functional crown types

Ecometrics is a trait-based approach based on the study of functional morphological features of organisms that attempts to quantify links between the distribution of those traits across biotic communities and specific environmental factors as well as to analyze their dynamics through space and time in the fossil record (Fortelius et al., 2002; Eronen et al., 2010b; Vermillion et al., 2018). Ecometric traits are measurable macroscopic features that are known to represent their function in relation to local environmental conditions (Eronen et al., 2010b)—either due to adaptive reasons or to use/plasticity (ecophenotypic features). The most typical ecometric traits of vertebrates describe dental morphology, limb proportions, and body mass. Candidate traits for ecometric modeling must be at least preliminarily known to be associated through their functional relationship with the local environmental conditions, including the dominant temperature, precipitation, or dominant vegetation type (Eronen et al., 2010b; Vermillion et al., 2018). However, the exact associations are captured computationally when fitting statistical models to link the traits of communities with their environmental conditions. Due to its functional perspective, ecometrics has sometimes been referred to as a taxon-free approach to highlight that the ecology of fossil organisms is not inferred from that of their nearest living relatives and that ecometric approaches do not rely on presence or absence of any particular individual taxa. Theoretically, ecometric approaches can be completely taxon blind—e.g., analyzing random samples of teeth that are found at localities without considering any taxonomic information. However, in practice, for robustness and potentially larger samples, most ecometric studies, including the present work, analyze the distribution of traits over species at localities, sometimes on global-scale datasets (e.g., Liu et al., 2012; Žliobaitė et al., 2018). Ecometrics, thus, does not focus on individual organisms but deals with the functional composition of communities, thereby enabling comparisons between present and past communities. Of course, there is no way to statistically test for predictions about the past (retrodictions), which makes it necessary to use different approaches and see how they compare. Because of its relatively fast and nondestructive sampling, dental ecometrics has been particularly used to make large-scale inferences about paleoenvironmental and biotic changes across different geographic and temporal scales, and different tailored global and regional models have been developed for different types of analysis (Eronen et al., 2010b; Liu et al., 2012; Fortelius et al., 2016; Žliobaitė et al., 2016; Oksanen et al., 2019).

**Table 1**

Summary of previous paleoenvironmental reconstructions of Can Llobateres 1 as compared to the present one, including methods, data analyzed, paleoenvironmental inferences, and references.

Reference	Methods and data analyzed	Paleoenvironmental inferences
Nagatoshi (1987)	Qualitative evaluation of fauna and flora	Habitat dominated by fringing forest and open woodland, followed by swamp forest and forest/grassland mosaic, and to a lesser extent parkland and grassland, with river/stream, lake, and marsh water sources
Andrews (1996)	Analysis of community structure using various methods	Classified as a subtropical seasonal forest
Hernández Fernández et al. (2003)	Multivariate analysis of faunal composition	Classified as a deciduous tropical forest with high probability
Costeur (2005)	Cenogram analysis	Considered a tropical forest with very closed and humid conditions
Casanovas-Vilar and Agustí (2007)	Multivariate analysis of the rodent assemblage	Considered a humid warm-temperate evergreen forest
Marmi et al. (2012)	Qualitative evaluation of plant remains	Habitat consisting of a marshy area surrounded by a dense wetland or riparian forest in a warm-temperate climate with high mean annual temperatures, probably with more open woodlands far from the wetlands

**Table 2**  
Updated list of the mammals from Can Llobateres 1.

Order	Family	Species <sup>a</sup>
Eulipotyphla	Erinaceidae	<i>Lantanothereum sanmigueli</i>
Eulipotyphla	Erinaceidae	<i>Parasorex</i> sp.
Eulipotyphla	Erinaceidae	cf. <i>Postpalerinaceus</i> sp.
Eulipotyphla	Dimylidae	<i>Plesiodimylus chantrei</i>
Eulipotyphla	Dimylidae	<i>Metacordylodon schlosseri</i>
Eulipotyphla	Talpidae	<i>Desmanella</i> sp.
Eulipotyphla	Talpidae	<i>Talpa vallesiensis</i>
Eulipotyphla	Talpidae	<i>Talpa</i> sp. 2
Eulipotyphla	Heterosoricidae	<i>Dinosorex grycivensis</i>
Eulipotyphla	Soricidae	<i>Miosorex grivensis</i>
Eulipotyphla	Soricidae	<i>Lartetium</i> sp.
Eulipotyphla	Soricidae	<i>Paenelimoecus</i> sp.
Eulipotyphla	Soricidae	<i>Crusafontina endemica</i>
Chiroptera	–	Chiroptera indet.
Lagomorpha	Ochotonidae	<i>Prolagus crusafonti</i>
Rodentia	Sciuridae	<i>Csakvaromys bredai</i>
Rodentia	Sciuridae	<i>Heteroxerus rubricati</i>
Rodentia	Sciuridae	<i>Albanensia</i> aff. <i>grimmi</i>
Rodentia	Sciuridae	<i>Miopetaurista neogrivensis</i>
Rodentia	Sciuridae	<i>Miopetaurista crusafonti</i>
Rodentia	Sciuridae	<i>Blackia miocaenica</i>
Rodentia	Sciuridae	cf. <i>Pliopetaurista</i> sp.
Rodentia	Castoridae	<i>Euroxenomys minutus</i>
Rodentia	Castoridae	<i>Chalicomys jaegeri</i>
Rodentia	Gliridae	<i>Glirudinus</i> cf. <i>undosus</i>
Rodentia	Gliridae	<i>Myoglis meini</i>
Rodentia	Gliridae	<i>Muscardinus vallesiensis</i>
Rodentia	Gliridae	<i>Muscardinus hispanicus</i>
Rodentia	Gliridae	<i>Bransatoglis astaracensis</i>
Rodentia	Gliridae	<i>Paraglrulus werenfelsi</i>
Rodentia	Gliridae	<i>Glirulus lissiensis</i>
Rodentia	Eomyidae	<i>Eomyops catalaunicus</i>
Rodentia	Eomyidae	<i>Keramidomys pertesunatoi</i>
Rodentia	Cricetidae	<i>Eumyarion lemanni</i>
Rodentia	Cricetidae	<i>Hispanomys thaleri</i>
Rodentia	Cricetidae	<i>Megacricetodon</i> cf. <i>minutus</i>
Rodentia	Cricetidae	<i>Democricetodon</i> cf. <i>nemoralis</i>
Rodentia	Cricetidae	<i>Cricetodon sabadellensis</i>
Rodentia	Cricetidae	<i>Anomalomys gaillardi</i>
Carnivora	Viverridae	<i>Semigenetta ripolli</i>
Carnivora	Barbourofelidae	<i>Albanosmilus jordani</i>
Carnivora	Felidae	<i>Machairodus aphanistus</i>
Carnivora	Hyaenidae	<i>Protictitherium crassum</i>
Carnivora	Amphicyonidae	<i>Amphicyon</i> sp.
Carnivora	Amphicyonidae	<i>Ammitocyon</i> sp.
Carnivora	Ursidae	<i>Ursavus brevirhinus</i>
Carnivora	Ursidae	<i>Miomaci</i> sp.
Carnivora	Ursidae	<i>Indarctos vireti</i>
Carnivora	Ailuridae	<i>Protursus simpsoni</i>
Carnivora	Mephitidae	<i>Mesomephitis medius</i>
Carnivora	Mustelidae	<i>Martes melibulla</i>
Carnivora	Mustelidae	<i>Circamustela dechaseauxi</i>
Carnivora	Mustelidae	<i>Marcetia santigae</i>
Carnivora	Mustelidae	<i>Trochictis narcisoi</i>
Carnivora	Mustelidae	<i>Eomellivora fricki</i>
Carnivora	Mustelidae	<i>Sabadellictis crusafonti</i>
Carnivora	Mustelidae	<i>Trocharion albanense</i>
Hyracoidea	Pliohyracidae	<i>Pliohyrax rossignoli</i>
Proboscidea	Deinotheriidae	<i>Deinotherium giganteum</i>
Proboscidea	Gomphotheriidae	<i>Tetralophodon longirostris</i>
Perissodactyla	Chalicotheriidae	<i>Chalicotherium goldfussi</i>
Perissodactyla	Equidae	<i>Hippotherium</i> cf. <i>primigenium</i>
Perissodactyla	Rhinocerotidae	<i>Alicornops simorreense</i>
Perissodactyla	Rhinocerotidae	cf. <i>Aceratherium incisivum</i>
Perissodactyla	Rhinocerotidae	<i>Dihoplus</i> cf. <i>schleiermachersi</i>
Perissodactyla	Tapiridae	<i>Tapirus priscus</i>
Artiodactyla	Suidae	<i>Listriodon splendens</i>
Artiodactyla	Suidae	<i>Parachleuastochoerus valentini</i>
Artiodactyla	Suidae	<i>Parachleuastochoerus crusafonti</i>
Artiodactyla	Suidae	<i>Propotamochoerus palaeochoerus</i>
Artiodactyla	Tragulidae	<i>Dorcatherium nauti</i>
Artiodactyla	Moschidae	<i>Micromeryx</i> aff. <i>flourensianus</i>
Artiodactyla	Bovidae	<i>Miotragocerus pannoniae</i>
Artiodactyla	Bovidae	<i>Protragocerus chantrei</i>

(continued on next page)

Table 2 (continued)

Order	Family	Species <sup>a</sup>
Artiodactyla	Cervidae	<i>Amphiprox anocerus</i>
Artiodactyla	Cervidae	Cervidae indet.
Artiodactyla	Giraffidae	Giraffidae indet.
Primates	Hominidae	<i>Hispanopithecus laietanus</i>

<sup>a</sup> Taxa included in the ecometric analyses are in bold.

In this study, we aim at predicting multiple climatic characteristics of CLL1, for which we use the dental trait scoring scheme reported in Žliobaitė et al. (2016), termed functional crown types (FCT). This scheme was devised to potentially increase the scope of environmental predictions particularly in the Late Miocene and Plio-Pleistocene. The scheme is based on a modular system called crown types (Jernvall, 1995), which was designed to be applicable to mammals generally, primarily focusing on the shape of unworn teeth. Functional crown types, in contrast, focus on characteristics of how teeth wear while in use. The FCT scheme includes seven variables (Žliobaitė et al., 2016; Galbrun et al., 2018). Ecometric approaches based on hypsodonty (HYP; relative crown height) and loph count (Fortelius et al., 2002, 2016; Eronen et al., 2010a, 2010c; Liu et al., 2012; Oksanen et al., 2019) have been used to estimate paleoprecipitation and productivity in the Old World from the Miocene through the Pleistocene, as well as temperature in the Pleistocene. However, the set of seven variables of the FCT scheme offers potential for estimating a broader set of climatic conditions, including seasonality characteristics and reoccurring extremities of climatic conditions (Žliobaitė et al., 2016). Here, we apply regional and global ecometric approaches based on the FCT of herbivorous large mammals from CLL1 to refine the previous paleoenvironmental inferences on the habitat of *H. laietanus*.

## 2. Materials and methods

### 2.1. Studied material

As in Žliobaitė et al. (2016), this study was restricted to herbivorous large mammals of the orders Artiodactyla, Perissodactyla, Proboscidea, and Primates and focused on M<sup>2</sup>s (see also Galbrun et al., 2018). We scored dental traits at the species level. An updated faunal list of the mammals recorded at CLL1, including 20 species of the aforementioned orders (Table 2), was compiled based on the information available from the Vallès-Penedès Miocene Vertebrates—Paleobiodiversity Database

(Casanovas-Vilar et al., 2018; Alba et al., 2022a), which includes specimen identification and provenance information for Miocene vertebrate remains from the Vallès-Penedès Basin and is maintained by ICP researchers, not yet openly accessible. The identification of multiple species was also revised in the course of this work by examining the original material housed in the ICP and comparing it with that from published sources. Functional crown-type variables were scored by visual inspection from M<sup>2</sup>s in all species of large herbivorous mammals. Žliobaitė et al. (2016) scored these variables from M<sup>3</sup>s in the case of African Suidae, where typically M<sup>3</sup> was the dominant molar for adults. However, this was not necessary in the case of the Miocene suid species recorded at CLL1, where the scores for M<sup>2</sup> and M<sup>3</sup> were the same. When the identification of a taxon was well documented in the literature and M<sup>2</sup>s were available from CLL1, we focused on this material to score the FCT variables. When any of these conditions did not apply, other dental (or even postcranial) remains were studied to confirm or refine the taxonomic identifications. When no M<sup>2</sup>s were available from CLL1 for a particular taxon, FCT variables were based on those of the same species or higher taxonomic ranks from elsewhere as reported in the literature.

### 2.2. Ecometric analysis

**Functional crown types** The FCT dental trait scoring scheme was designed to capture main functional traits (durability, cutting, and other occlusal properties, as well as dental tissues) of tooth shape and worn occlusal surfaces of herbivorous large mammal teeth, based on seven (two ordinal and five binary) variables (Žliobaitė et al., 2016; Galbrun et al., 2018) that are summarized in Table 3. The two ordinal variables, HYP and horisodonty (HOD; length of the functional occlusal surface in terms of main cusp pairs), are related to tooth durability and have three states each (Table 3). In turn, the binary variables record three additional functional aspects (Table 3), namely cutting structures (acute lophs [AL] and obtuse, or basin-like, lophs [OL]); occlusion characteristics (structural fortification [SF] of cusps and occlusal topography

**Table 3**  
Definition and scoring of functional crown type variables following Žliobaitė et al. (2016).

Variable	Abbreviation	Definition	Scoring			
			0	1	2	3
Hypsodonty	HYP	Height of a tooth crown relative to its length <sup>a</sup>		Brachyodont	Mesodont	Hypsodont
Horisodonty	HOD	Length of the functional occlusal surface (number of main cusp pairs along the mesiodistal axis) <sup>b</sup>		Brachyhorisodont	Mesohorisodont	Hypsohorisodont
Acute lophs	AL	Sloped linear structures typically having straight edges	Absent	Present		
Obtuse lophs	OL	Nonsloped linear structures that typically have curved edges	Absent	Present		
Structural fortification of cusps	SF	Structures that strengthen and reinforce the cusps (usually by differential thickness of enamel)	Absent	Present		
Occlusal topography	OT	Lack (flat) or presence (nonflat) of occlusal raised elements such as cusps <sup>c</sup>	With raised elements	Flat		
Coronal cementum	CM	Presence or absence of thickened cementum in the crown, supporting its strength and durability	Absent or very thin	Thick coating		

Abbreviations: HYP = hypsodonty; HOD = horisodonty; AL = acute lophs; OL = obtuse lophs; SF = structural fortification; OT = occlusal topography; CM = coronal cementum.

<sup>a</sup> Hypsodonty categories (Fortelius et al., 2002; Žliobaitė et al., 2016; Galbrun et al., 2018): brachyodont = lower than long (<0.8); mesodont = approximately as tall as long (0.8–1.2); hypsodont = taller than long (>1.2).

<sup>b</sup> Horisodonty categories (Žliobaitė et al., 2016): brachyhorisodont = 1–2 cusp pairs; mesohorisodont = 3 cusp pairs; hypsohorisodont = more than 3 cusp pairs.

<sup>c</sup> Lophodont teeth can be flat or non-flat.

[OT]); and material properties (coronal cementum [CM]). Based on data from extant environments (national parks) from Kenya, these variables have been shown to be correlated with environmental (climatic and ecological) parameters—such as precipitation (PREC), temperature (TEMP), net primary productivity (NPP), and normalized difference vegetation index (NDVI; i.e., the greenness of the vegetation)—thus being promising for making paleoenvironmental inferences based on fossil data (Žliobaitė et al., 2016).

To retrace the paleoenvironmental conditions of CLL1, we scored the seven FCT variables for the herbivorous large mammal species present at this locality and, based on the average for each variable, we followed the two different approaches described below. While FCT scoring scheme has remained fixed over the years, scoring conventions of selenodonts have changed from Oksanen et al. (2019) onward. For compatibility with the predictive models used in our first approach, here we use the scoring conventions as they were defined in Žliobaitė et al. (2016), scoring all selenodonts with OL and the Furchen of suids as fortified.

**First approach** Based on the seven FCT variables scored for 13 sites in Kenyan national parks, Žliobaitė et al. (2016) derived predictive models for 23 environmental (climatic and ecological) variables using least angle regression, which uses an iterative procedure to select the most informative dental trait predictors (while avoiding redundancies). The resulting regression models, to be used for predictive purposes, take the same functional form as ordinary linear regression (a linear combination of input variables). In our first approach, we used the 23 regression models (based on three FCT variables each) reported by Žliobaitė et al. (2016: Table 2; see our [Supplementary Online Material \[SOM\] Table S1](#)) to estimate 23 paleoenvironmental variables at CLL1. These regression models were not optimized for predictive purposes but rather for comparability of information content in different seasonality indices, using a constant number of trait variables in each model. Yet, those models were tested for predictive accuracy at the present day and in principle can be used for analysis of the fossil record.

An obvious limitation of this approach is that the regression models are regional, calibrated on present day Kenya—no comparable models are available from elsewhere—which is not necessarily representative of past environments during the Iberian Miocene. On the other hand, the geographically restricted nature of the dataset could also potentially result in a greater optimization of the regression equations used to estimate the paleoenvironmental parameters. In any event, we consider that the scope of the environments covered by the Kenyan localities used to derive the models is compatible with a range of environments that can potentially be expected at CLL1 and, thus, is applicable to this fossil locality. Furthermore, precisely because of the aforementioned limitation, we also followed an alternative approach that was not based on such models but on the covariation between FCT variables and biomes in a much less geographically restricted dataset.

**Second approach** As an alternative approach, we used principal component analysis (PCA) and canonical variate analysis (CVA) performed with R v. 4.1.1 (R Core Team, 2021) through Rstudio v. 2021.9.0.351 (RStudio Team, 2021) to evaluate to what extent FCT variables discriminate among different types of biomes and can be reliably used to make such inferences.

First, we used the Whittaker's system of present-day biomes to classify the 13 sites in Kenyan national parks from Žliobaitė et al. (2016), based on their mean annual temperature (MAT) and mean annual precipitation (MAP) into the different biomes of the world characterized according to the distribution of vegetation types (Whittaker, 1975). We plotted them in the Whittaker biomes diagram using the R packages 'devtools' v. 2.4.3 (Wickham et al., 2021), 'plotbiomes' v. 0.0.0.9001 (Stefan and Levin, 2022), and 'ggplot2' v. 3.3.5 (Wickham, 2016) and performed a PCA with not normalized input variables (i.e., the average values for each FCT variable at each locality) using the R packages 'ade4' v. 1.7.18 (Chessel et al., 2004; Dray and Dufour, 2007; Dray et al., 2007; Bougeard and Dray, 2018; Thioulouse et al., 2018),

'factoextra' v. 1.0.7 (Kassambara and Mundt, 2020), and 'ggplot2' v. 3.3.5 (Wickham, 2016).

Second, we also relied on a geographically much wider dataset of FCT variables to further assess if they are useful to correctly classify extant localities according to Whittaker biomes using a CVA based on FCT data. In particular, we used Galbrun et al.'s (2018) dataset (available online at <https://github.com/zliobaite/teeth-redescription>), which contains data from 28,886 localities around the world on environmental variables, species composition, and FCT variables for each species. We extracted the average of each FCT variable for those localities that, according to the Whittaker diagram, correspond to certain biomes that, based on previous literature (see Table 1), seem relevant to compare with CLL1 (temperate rainforest, temperate seasonal forest, tropical rainforest, tropical seasonal forest/savanna, and woodland/shrubland). The FCT variables mean HYP and mean HOD were provided as three separate binary variables each in Galbrun et al.'s (2018) dataset but were transformed back to ordinal variables for this study. Once the localities were classified, we performed a cross-validated CVA on the same data, using biomes to distinguish a priori groups, with the R packages 'Morpho' v. 2.9 (Schlager, 2017) and 'ggplot2' v. 3.3.5 (Wickham, 2016). To better evaluate the structuration of the data and be able to discount spurious group separation, we computed the amount of variance ( $r^2$ ) explained by group differences in the raw data and the CVA (with and without cross-validation), using a permutational multivariate analysis of variance (1000 permutations) with the R package 'RRPP' v. 1.3.1 (Collyer and Adams, 2018, 2019). Percentages of correct classification were computed based on the cross-validated CVA.

Finally, based on the CVA, CLL1 and the Kenyan localities were classified according to Whittaker's biomes. The probability that each locality belongs to one of the biomes distinguished a priori was evaluated based on the standard posterior probabilities of group membership (which add up to 1 when all the biomes distinguished a priori are considered) as well as the typicality probabilities (which test if a given locality falls outside the variation of each biome independently). To evaluate the consistency of the results for CLL1, the biome classification favored by the CVA posterior probabilities was compared with that obtained from the estimates of paleotemperature and paleoprecipitation yielded by the regressions based on FCT average values in our first approach. To further assess the reliability of the classification provided by the CVA for CLL1, the classification for the nine Kenyan sites from Žliobaitė et al. (2016) corresponding to the five relevant biomes included in the CVA was also compared with that obtained from actual data on temperature and precipitation.

### 3. Results

**Species identification** An updated list of mammals from CLL1 is reported in Table 2. The herbivorous large mammals included in FCT analyses include 20 species from 19 genera and 13 families, whereas the complete mammal list includes 78 species (39 small and 39 large mammals). While a few small mammal species are added here, the number of large mammal species from CLL1 (39) reported in Table 2 is lower than the figure of 47 species reported by Alba et al. (2011a) and even the figure of 41 currently recognized by the New and Old Worlds database (The NOW Community, 2023). All these changes are not attributable to recovery of new taxa during the new campaigns since 2010 but rather to the ongoing revision of the collections recovered in previous decades.

With regard to micromammals, the most updated list of eulipotyphlans from CLL1 is probably that reported by Van den Hoek Ostende and Furió (2005). The current list differs in the following regards: (1) the galericine previously assigned to *Parasorex socialis* is attributed to *Parasorex* sp., pending illumination of the relationship between *Parasorex ibericus* and the central European '*Schizogalerix*' *voesendorfensis* Cailleux et al. (in press); (2) the erinaceid previously attributed to *Postpalerinaceus vireti* by Crusafont Pairó and Gibert Clocs (1974) is

considered to represent a different species (tentatively referred to cf. *Postpalerimaceus* sp.); (3) besides *Talpa vallesiensis*, two additional talpids (*Desmanella* sp. and *Talpa* sp.) are recorded; (4) the heterosoricid present at the site is *Dinosorex grycovensis* instead of *Dinosorex sansaniensis* (see Furió et al., 2015); and (5) an additional dimyloid (*Metacordylodon schlosseri*) and three additional soricids (*Miosorex grivensis*, *Lartetium* sp., and *Paenelimnoecus* sp.) are identified. An indeterminate chiropteran and a single lagomorph (contra Alba et al., 2011a) are also identified at CLL1. As for the rodents, the list is taken from Casanovas-Vilar et al. (2016b), and only the genus ascription of *Csakvaromys bredai* has been updated following Sinitza et al. (2022).

Regarding the macromammals from CLL1 not included in the FCT computations, most changes correspond to carnivorans. Their list is based on the review by Robles et al. (2014), with several subsequent updates: (1) no material of *Promephitis pristinidens* has been identified, and it is thus considered that previous citations of this genus from CLL1 correspond to *Mesomephitis medius*; (2) *Hoplictis petteri* is considered a junior subjective synonym of *Eomellivora fricki* following Valenciano et al. (2019); (3) a single hyaenid (*Protictitherium crassum*) is recognized from CLL1; (4) the two amphicyonids from the site, currently under study, are provisionally attributed to *Amphicyon* sp. and *Ammitocyon* sp.; and (5) three ursids are recorded, but instead of two *Ursavus* species, only *Ursavus brevirhinus* is present at the site, with scarce dental material being attributable instead to *Miomaci* sp.—an indarctin ursid genus present at Rudabánya and Can Poncic (de Bonis et al., 2017). In addition, the hyracoid is assigned to *Pliohyrax rossignoli* following Pickford et al. (1997), although more detailed comparisons of the scarce material available would be required to confirm such an attribution. The remaining large mammals are those included in the FCT analyses and hence are discussed in greater detail in the following paragraphs, as they constitute the basic information needed to replicate our results. An argument could be made that hyraxes should be included in the FCT computations, but we decided to exclude them as they were not considered in the equations originally derived by Žliobaitė et al. (2016).

Two proboscidean species are recorded: a deinotherid and a gomphotherid. The deinotheriid remains from CLL1 were described by Bergounioux and Crouzel (1962), who attributed them to *Deinotherium giganteum*, which is currently considered the only deinotheriid species present in MN9 of Europe (e.g., Pickford and Pourabrishami, 2013; Alba et al., 2020). The gomphotheriid remains were described by Mazo (1977), who attributed them *Tetralophodon longirostris*, which replaced *Gomphotherium angustidens* in late MN7+8 (Mazo and Van der Made, 2012).

Perissodactyls are represented at CLL1 by six species (a chalicotherid, a horse, three rhinoceroses, and a tapir). The chalicotheriid remains are unpublished but were reported as *Chalicotherium grande* (currently *Anisodon grande*) by Mein (1990) and were later reassigned to *Chalicotherium goldfussi* by Heissig (1999). The latter assignment is confirmed here, based on the position of the M<sup>1</sup> and M<sup>2</sup> metacones (see Anquetin et al., 2007), in further agreement with the MN9 age of the site (the two species only overlap in late MN7+8; Anquetin et al., 2007). The equid remains were attributed to *Hipparion primigenium primigenium* by Alberdi (1974). Following Bernor et al. (1980, 1996, 2021), these remains could be assigned to a distinct species endemic of the Vallès-Penedès Basin (*Hippotherium catalaunicum*). However, a long-needed revision of the Vallès-Penedès *Hippotherium* remains has been undertaken by some of the authors of this paper, and on this basis, we prefer to tentatively assign the CLL1 remains to *Hippotherium* cf. *primigenium*. This is because differences with the vast sample of this species from Höwenegg (Bernor et al., 1997, 2022), at present time, do not seem to warrant a species distinction. The rhinocerotid remains from CLL1, in turn, were described by Santafé Llopis (1978), being attributed to four species, whose genus attribution has been updated based on Sanisidro and Cantalapiedra (2022). Although these authors reported four species from CLL1, we refrained from including *Lartetotherium sansaniense* because its identification by Santafé Llopis (1978) relies on a single damaged scaphoid that

displays aceratheriine affinities. A preliminary revision of the remains from the other rhinocerotid species by one of the authors of this paper further indicates that more in-depth revision is required. On the one hand, the species attribution of the *Dihoplus* remains must be considered tentative because they show some dental differences as compared with *Dihoplus schleiermacheri* from Central Europe. For the same reason, the identification of *Aceratherium incisivum* is even more tentative, and the remains might even belong to a different genus as they display some dental features that fall outside the normal variation of the genus as recorded in Central Europe. Finally, the tapirid remains were described by Golpe-Posse and Crusafont-Pairó (1982), who attributed them to *Tapirus priscus*, an attribution that is confirmed here.

Artiodactyls are more diverse than perissodactyls, being represented at CLL1 by 11 species (four suids, a tragulid, a moschid, two bovids, two cervids, and a giraffid), although only the suid *Parachleuastochoerus crusafonti*, the bovid *Miotragocerus pannoniae*, and at least one of the cervids are common faunal elements. The suid remains were described by Golpe-Posse (1971, 1972), who recognized four different species: *Listriodon splendens*, *Pa. crusafonti*, *Hyotherium soemmeringi*, and ?*Hyotherium* sp. Pickford (1981, 2014) provided additional descriptions of the *Pa. crusafonti* sample from CLL1, which is the type locality of the species. The identification of *L. splendens* at CLL1 by Golpe-Posse (1971, 1972) was based on two teeth, a purported molar and a premolar, the latter being assigned by the same author to ?*Hyotherium* sp. The revision of the material indicates that the former belongs in fact to *T. priscus* and that the latter to *Pa. crusafonti*. However, two infantile specimens reported by Van der Made (1996) and a few additional unpublished deciduous teeth confirm the presence of *L. splendens* at CLL1, representing the last well-dated occurrence of the genus in Europe (Van der Made et al., 2022). The larger-bodied tetraconodontine from CLL1 identified by Golpe-Posse (1971, 1972) as *Hy. soemmeringi* was later reassigned to *Conohyus steinheimensis* by Van der Made (1990). The species was later included in *Parachleuastochoerus steinheimensis* and, more recently, was split into *Versoporcus steinheimensis* and *Versoporcus grivensis* by Pickford (2014, 2016). However, the revision of the single premolar attributed by Golpe-Posse (1971, 1972) to *Hy. soemmeringi* indicates that, together with an incisor, it belongs to the larger tetraconodontine referred by Pickford (2014, 2016) to *Parachleuastochoerus valentini* (see also McKenzie et al., 2023). The presence of a suine at CLL1 was first reported by De Bruijn et al. (1992) as *Korynochoerus palaeochoerus* (currently *Propotamochoerus palaeochoerus*; e.g., Van der Made et al., 1999; McKenzie et al., 2023), apparently based on unpublished material not yet available to Golpe-Posse (1971, 1972). The revision of the suid remains from CLL1 unambiguously confirms the presence of the species based on diagnostic dentognathic material.

The tragulid remains from CLL1, originally reported as *Dorcatherium* sp. (Crusafont Pairó, 1958), were subsequently identified as *Dorcatherium naui* by Moyà-Solà (1979; see also Alba et al., 2011c). The material is scanty and consists of a few tarsal bones and an upper canine. The even scarcer moschid remains from CLL1 are unpublished. Based on their small size and some details of occlusal morphology, they are referred to *Micromeryx* aff. *flourensianus* but probably belong to an undescribed species. The bovid remains from CLL1 were described by Moyà-Solà (1983) as *Protragocerus* aff. *chantrei* and *Miotragocerus* aff. *pannoniae*, but we concur with previous authors (e.g., Alba et al., 2011a) that open nomenclature (aff.) is unnecessary for these attributions, which are not tentative. The cervid remains from CLL1 have not been described in detail but were assigned to *Amphiprox anocerus* by Azanza and Menéndez (1990). Our review of the abundant material available from CLL1 indicates that dental variation would be compatible with the presence of a single species. However, the variation displayed by the antler material strongly suggests the presence of a second species, the taxonomic identity of which cannot be clarified at the moment—although an assignment to *Euprox dicranocerus*, present in earlier Vallesian sites (Azanza and Menéndez, 1990), seems unlikely. The giraffid remains from CLL1 were described by Crusafont Pairó

**Table 4**

Scoring of the functional crown types variables for the species of herbivorous large mammals recorded from Can Llobateres 1 (based on the  $M^2$ ) and average value computed for each variable.<sup>a</sup>

Species	HYP	HOD	AL	OL	SF	OT	CM
<i>Deinotherium giganteum</i>	1	1	1	0	0	0	0
<i>Tetralophodon longirostris</i>	1	3	0	1	0	0	0
<i>Chalicotherium goldfussi</i>	1	1	1	0	0	0	0
<i>Hippotherium cf. primigenium</i>	3	1	0	1	0	1	1
<i>Alicornops simorreense</i>	1	1	1	1	0	0	0
<i>cf. Aceratherium incisivum</i>	1	1	1	1	0	0	0
<i>Dihoplus cf. schleiermacheri</i>	1	1	1	1	0	0	0
<i>Tapirus priscus</i>	1	1	1	0	0	0	0
<i>Listriodon splendens</i>	1	1	1	0	0	0	0
<i>Parahcleuastochoerus valentini</i>	1	1	0	0	1	0	0
<i>Parahcleuastochoerus crusafonti</i>	1	1	0	0	0	0	0
<i>Propotamochoerus palaeochoerus</i>	1	1	0	0	1	0	0
<i>Dorcatherium naui</i>	1	1	0	1	0	0	0
<i>Micromeryx aff. flourensianus</i>	1	1	0	1	0	0	0
<i>Miotragocerus pannoniae</i>	2	1	0	1	0	0	0
<i>Protragocerus chantrei</i>	1	1	0	1	0	0	0
<i>Amphiprox anocerus</i>	1	1	0	1	0	0	0
Cervidae indet.	1	1	0	1	0	0	0
Giraffidae indet.	1	1	0	1	0	0	0
<i>Hispanopithecus laietanus</i>	1	1	0	0	0	0	0
Mean	1.150	1.100	0.350	0.600	0.100	0.050	0.050

Abbreviations: HYP = hypsodonty; HOD = horisodonty; AL = acute lophis; OL = obtuse or basin-like lophis; SF = structural fortification of cusps; OT = occlusal topography; CM = coronal cementum.

<sup>a</sup> The scoring protocol of Žliobaitė et al. (2016) is followed (no acute lophis are scored for selenodonts). See the Materials and methods for details about the meaning of each score.

**Table 5**

Estimates of 23 environmental variables for Can Llobateres 1 based on the regressions published by Žliobaitė et al. (2016)<sup>a</sup> and the functional crown type variables computed in this study for Can Llobateres 1 (Table 4).

Paleoenvironmental variable	Estimates for CLL1
<b>Mean annual precipitation (MAP)<sup>b</sup></b>	<b>881 mm</b>
Driest month over year	136 mm
Driest place over year	974 mm
Wettest month over year	2119 mm
Wettest place over year	816 mm
Average annual NPP	1352 g C/m <sup>2</sup>
Coldest and driest month over year	174 g C/m <sup>2</sup>
Coldest days with driest place	1090 g C/m <sup>2</sup>
Coldest days with driest month	182 g C/m <sup>2</sup>
Coldest month driest place over year	1257 g C/m <sup>2</sup>
Average NDVI	0.91
Global minimum over 9 yr	0.60
Average over yearly minimums	0.67
Minimum over yearly averages	0.68
Average over monthly minimums	0.85
Minimum over monthly minimums	0.74
<b>Mean annual temperature (MAT)<sup>b</sup></b>	<b>25 °C</b>
Coldest month over year	24 °C
Average over coldest days of months	17 °C
Minimum over coldest days of months	17 °C
Hottest month over year	27 °C
Average over hottest days of months	30 °C
Maximum over hottest days of months	34 °C

Abbreviation: NDVI = normalized difference vegetation index; NPP = net primary productivity; CLL1 = Can Llobateres 1.

<sup>a</sup> See SOM Table S1 for the parameters of Žliobaitė et al.'s (2016: Table 2) regressions. The variables used in Whittaker's biome attribution are bolded.

<sup>b</sup> These variables were termed annual precipitation and average temperature in Žliobaitė et al. (2016).

(1952), who assigned them to *Palaeotragus* sp. Here, however, they are merely referred to Giraffidae indet. because the available material merely consists of a few isolated postcranial elements that do not allow for a species or genus attribution, particularly taking into account the taxonomic uncertainties about the MN9 giraffids from the Vallès-Penedès Basin (Alba et al., 2022b).

Finally, as explained in greater detail in the Introduction, the

hominid remains from CLL1 were first reported by Crusafont-Pairó (1958). The material currently available was described in detail by Begun et al. (1990), Golpe-Posse (1993), and Alba et al. (2012a). Although Crusafont Pairó and Hürzeler (1961, 1969) and subsequently Golpe-Posse (1993) recognized the presence of various species, currently, the whole sample is attributed to *H. laietanus* (Alba, 2012; Alba et al., 2012a). Nevertheless, based on enamel–dentine shape, the presence of a second hominoid species at CLL1 cannot be entirely ruled out (Zanolli et al., 2023).

**Paleoenvironmental estimates based on the first approach** The values for the FCT variables for the investigated species recorded at CLL1 are reported in Table 4, while the 23 estimated environmental variables for this site are reported in Table 5. Most noteworthy are the estimated values of paleotemperature (MAT = 25 °C) and paleoprecipitation (MAP = 881 mm), which indicate a Whittaker's biome of tropical seasonal forest/savanna for CLL1 (Fig. 2).

**Paleoenvironmental estimates based on the second approach** The first two principal components (PCs) of a PCA based on FCT variables for 13 extant localities from Kenyan national parks (Fig. 3) summarize more than 75% of the variance. The PC1 (56% of the variance) is mostly driven by SF and AL toward negative scores, and the remaining FCT variables toward positive scores. The site of CLL1 displays very high scores along this axis, most similar to the extant localities of Shimba Hills (tropical seasonal forest/savanna) as well as Elgon and Kakamega (temperate seasonal forests). Along PC1, these three extant localities fall far from the rest of extant localities, which cluster close to one another despite corresponding to the four different biomes included in the analysis. The PC2 (21% of the variance) is mostly driven by SF (and, to a lesser extent, CM and HYP) toward negative scores, and by AL (and, to a much lesser extent, OT and OL) toward positive scores. Extant Kenyan localities corresponding to the temperate seasonal forest and woodland/shrubland biomes tend to display lower PC2 scores than those representing the tropical seasonal forest/savanna and subtropical desert biomes. The site of CLL1 displays an extremely positive score along this axis, well beyond any of the extant localities, suggesting relevant environmental differences even compared with the closest extant localities in PC1.

The CVA based on 18,671 extant localities from five different biomes accounts for 33.7% of the differences among the groups, which are

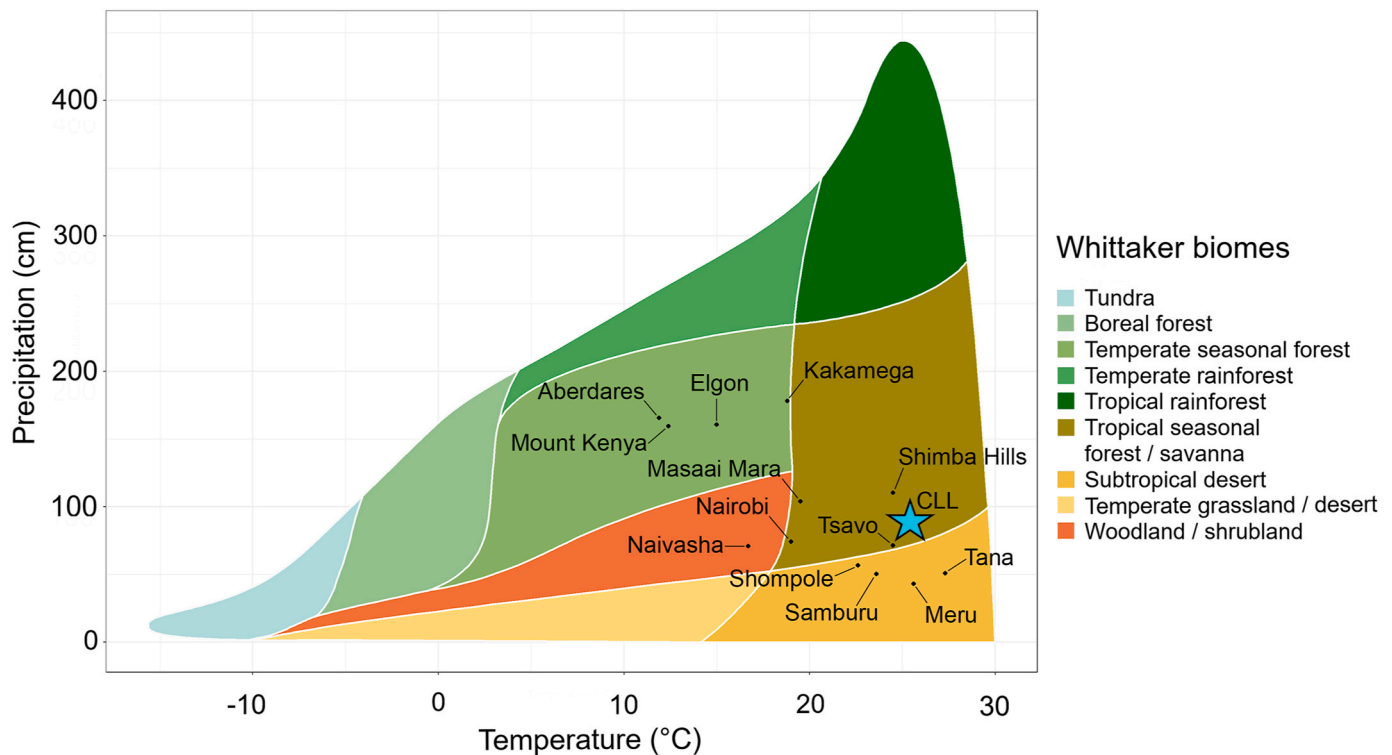


**Figure 2.** Whittaker's diagram with biome classification for Can Llobateres 1 (blue star) based on estimated paleotemperature and paleoprecipitation (Table 5), along with the nine extant localities from Kenyan national parks based on actual temperature and precipitation data (Zliobaitė et al., 2016). (For interpretation of the references to color in this figure legend, the reader is referred to the Web version of this article.)

statistically significant at  $p < 0.001$ , both with and without cross-validation. Differences among the groups are also statistically significant ( $p < 0.001$ ) based on the raw data—indicating that grouping structure is not spurious—although they explain a lower amount of variance (13.9%). The cross-validated CVA has a low classification accuracy (49.5% after cross validation; Table 6) because there is a considerable overlap among several biomes (Fig. 4). The first canonical variate (CV1) summarizes most of the variance (96%), being mostly determined by OL and, to a lesser extent, CM toward positive scores, and in decreasing order of importance, HOD, AL, and HYP toward negative scores. The analysis discriminates well between woodland/shrubland and tropical rainforest localities, and also quite well between the former and tropical seasonal forest/savanna localities (only with slight overlap of their 95% confidence ellipses). However, there is considerable overlap among these and other biomes, with the ellipse of the tropical rainforest biome being totally included within those of both the temperate rainforest and the tropical seasonal forest/savanna biomes, and further partly overlapping with that of the temperate seasonal forest biome. The second canonical variate (CV2) is positively driven by most of the variables to some extent, except OL (which has no influence) and AL (which has a moderate influence toward negative scores). Given the small amount of variance summarized by CV2 (3.5%), it is questionable whether it needs to be interpreted, as further confirmed by the fact that all the five investigated biomes overlap along this axis. However, it is noteworthy that the tropical rainforest biome shows a lower range of variation than the remaining ones, with all the localities included displaying negative scores for both CV1 and CV2. The locality of CLL1 also displays moderately negative scores for both axes, falling within the overlap zone among the ellipses of tropical seasonal forest/savanna, temperate rainforest, and tropical rainforest, and at the fringe of temperate seasonal forest.

However, based on the posterior probabilities (Table 7)—which hold assuming that the distribution of possible climatic conditions in the past is similar to that of the reference dataset of the present day—CLL1 is

classified as a tropical rainforest as a first option (63%) and as a tropical seasonal forest/savanna as second option (30%). The typicality probabilities (Table 7) are consistent with such classifications and confirm that, based on FCT variables, CLL1 statistically differs from all the remaining biomes at least with  $p < 0.05$ . The second classification option for CLL1 (tropical seasonal forest/savanna) according to the CVA based on FCT variables coincides with the biome attribution of our first approach—i.e., based on estimated paleotemperature and paleoprecipitation using Zliobaitė et al.'s (2016) regressions. Estimates of paleotemperature and paleoprecipitation are based on different sets of variables (OL, SF, and OT vs. HOD, SF, and OT, respectively) than those that have greater loadings on CV1 (OL, HOD and, to a lesser extent, AL and HYP), so it is not surprising that the classification results yielded by these two different approaches do not completely match. However, it is remarkable that the second classification option obtained from the CVA, with a lower posterior probability (30%), does coincide with the biome classification obtained from paleotemperature and paleoprecipitation estimates based on FCT variables. The biome classification results for the extant Kenyan localities based on the CVA only coincide with those based on actual data of temperature and precipitation in five out of nine cases (Table 8), which is not surprising, given the classification accuracy of the analysis around 50%. The mismatches correspond to localities from the temperate seasonal forest biome that are erroneously classified by the CVA as tropical seasonal forest/savanna, whereas the four localities actually corresponding to tropical seasonal forest/savanna are (like CLL1) correctly classified as such. It must be taken into account, however, that none of the localities from Kenyan national parks correspond to the tropical rainforest biome. The percentages of correctly classified cases for the 18,671 localities included in the CVA (Table 6) indicate that localities from the tropical seasonal forest/savanna biome are frequently erroneously classified as tropical rainforest (indeed, which the same frequency as the former are correctly classified, 42%), whereas tropical rainforest localities are most frequently correctly classified as such (82% of the cases) and misclassified as tropical

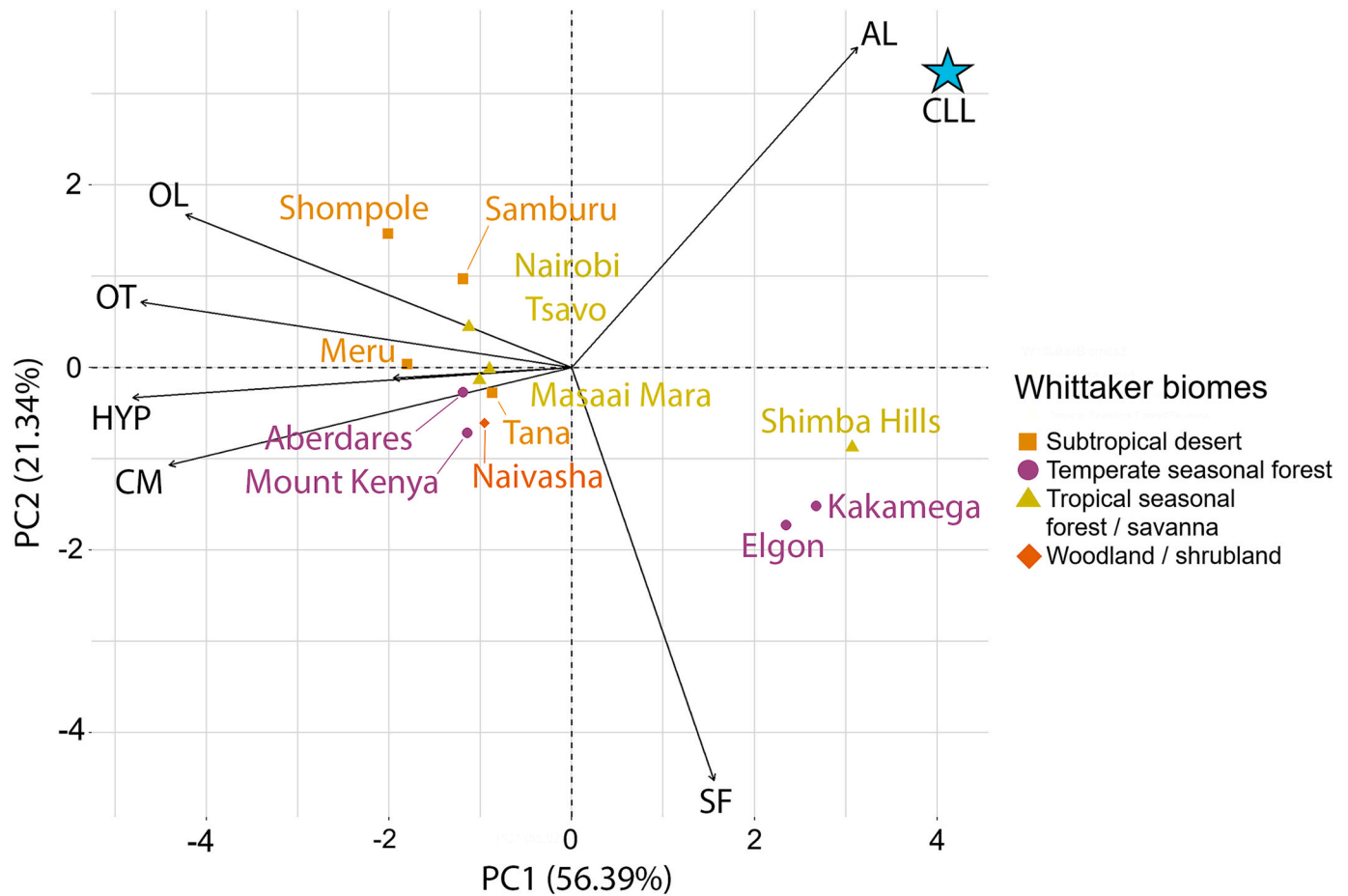


**Figure 3.** Results of a principal component (PC) analysis based on the seven functional crown type (FCT) variables of 13 extant localities from Kenyan national parks from four different biomes and Can Llobateres 1 (blue star), as depicted by a bivariate plot of PC2 vs. PC1. The percentage of variance summarized by each axis is indicated within parentheses. Vectors represent the loadings of the seven FCT variables (average values) on each axis. Each locality is color-coded according to Whittaker biome classification (see legend). Abbreviations: HYP = hypsodonty; HOD = horizodonty; AL = acute loph; OL = obtusate loph; SF = structural fortification; OT = occlusal topography; CM = coronal cementum. (For interpretation of the references to color in this figure legend, the reader is referred to the Web version of this article.)

**Table 6**

Summary classification results (in %) for the selected 18,671 extant localities from five Whittaker biomes based on the canonical variate analysis of seven functional crown type variables with cross-validation.<sup>a</sup>

	Temperate rainforest	Temperate seasonal forest	Tropical rainforest	Tropical seasonal forest/savanna	Woodland/shrubland
Temperate rainforest	<b>43.2</b>	4.9	29.6	9.9	12.4
Temperate seasonal forest	22.4	<b>23.7</b>	7.9	5.6	40.4
Tropical rainforest	8.8	0.3	<b>81.5</b>	9.4	0.1
Tropical seasonal forest/savanna	14.0	1.9	42.1	<b>41.7</b>	0.4
Woodland/shrubland	6.5	16.4	0.7	3.6	<b>72.8</b>

<sup>a</sup> Correct classification percentages after cross-validation are bolded.

rainforest/savanna with a low frequency (9%).

#### 4. Discussion

Environmental estimates and biome classification based on functional crown type variables The 23 prediction equations for environmental variables reported by Žliobaitė et al. (2016) vary in both accuracy ( $r^2$ , measuring the goodness of fit) and predictive power ( $r^{2*}$ , as measured by cross-validation). The former values vary from ~0.6–0.8 in the most reliable variables to less than 0.3 in the least ones, resulting in highly divergent equations in terms of their potential predictive power. While these models were not optimized to maximize the predictive accuracy, the calibration accuracy is reasonable for trying them

for predictive purposes on the fossil record. Probably, more accurate equations could be derived in the future based on a higher number of extant localities. In the meantime, the paleoenvironmental estimates derived from these equations for CLL1 should be taken with care as rough approximations whose reliability depends on the accuracy of the equations used to derive them. In other words, these estimates should not be taken at face value because the model calibration accuracy (or goodness of fit,  $r^2$ ) and, especially, the predictive power of these equations (calibration accuracy as measured by cross-validation,  $r^{2*}$ ) are quite low, and there is no guarantee that the Kenyan extant localities used to derive the models are representative of European environments during the Miocene. Nevertheless, the estimated parameters could be useful in relative terms to compare CLL1 with other well-sampled fossil

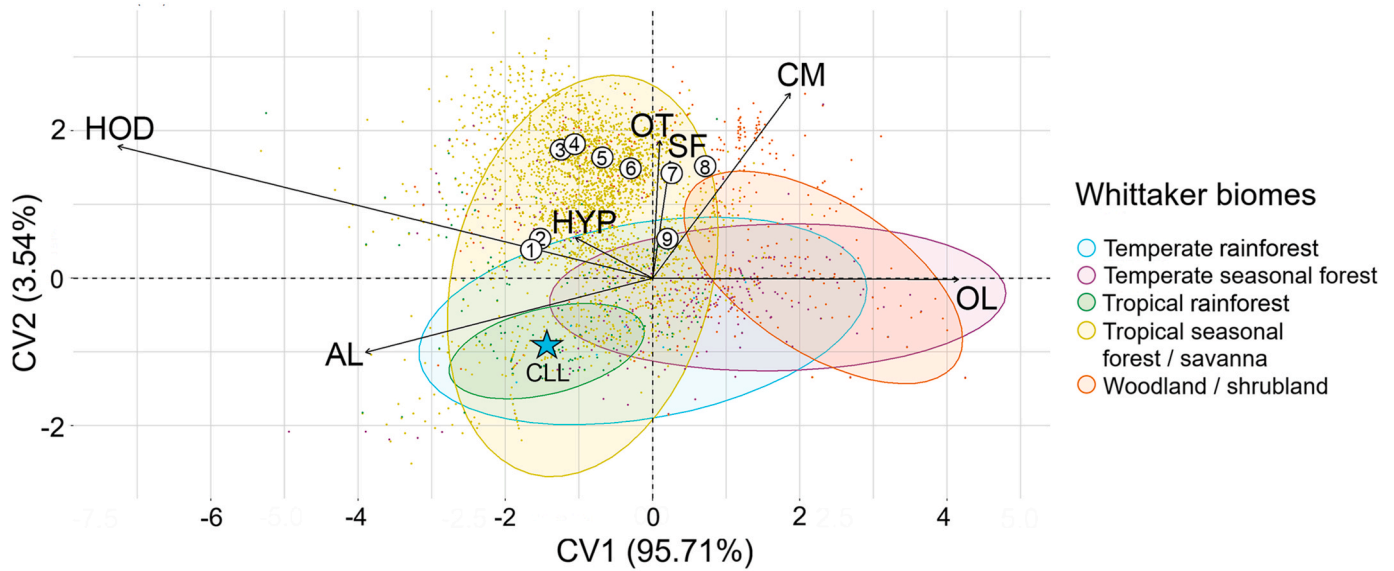


**Figure 4.** Results of a canonical variate (CV) analysis based on the seven functional crown type (FCT) variables of 18,671 extant localities from five different Whittaker biomes, as depicted by a bivariate plot of CV2 vs. CV1. The percentage of variance summarized by each axis is indicated within parentheses. Vectors represent the loadings of the seven FCT variables (average values) on each axis. Each locality is color-coded according to Whittaker biome classification (see legend). Ellipses represent the 95% confidence interval of each group included a priori. The nine localities from Kenyan national parks classified by this analysis, together with Can Llobateres 1 (blue star), are also depicted. Kenyan localities: 1 = Shimba Hills; 2 = Kakamega; 3 = Aberdares; 4 = Mt Kenya; 5 = Masaii Mara; 6 = Tsavo; 7 = Nairobi; 8 = Naivasha; 9 = Elgon. Abbreviations: HYP = hypsodonty; HOD = horisodonty; AL = acute lophs; OL = obtuse lophs; SF = structural fortification; OT = occlusal topography; CM = coronal cementum. (For interpretation of the references to color in this figure legend, the reader is referred to the Web version of this article.)

**Table 7**

Posterior probabilities and typicality probabilities for each Whittaker’s biome based on the canonical variate analysis of functional crown type variables for Can Llobateres 1 and nine extant localities from Kenyan national parks (Zliobaité et al., 2016).<sup>a</sup>

Locality	Temperate rainforest	Temperate seasonal forest	Tropical rainforest	Tropical seasonal forest/savanna	Woodland/shrubland
Posterior probabilities					
Aberdares	0.087	0.011	0.094	<b>0.806</b>	0.002
Elgon	0.245	0.210	0.092	<b>0.353</b>	0.100
Kakamega	0.116	0.009	0.230	<b>0.644</b>	0.001
Masaii Mara	0.157	0.025	0.099	<b>0.705</b>	0.013
Mt Kenya	0.090	0.013	0.096	<b>0.796</b>	0.004
Nairobi	0.228	0.104	0.067	<b>0.419</b>	0.181
Naivasha	0.187	0.195	0.025	0.222	<b>0.371</b>
Shompole	0.126	0.004	0.316	<b>0.553</b>	0.000
Tsavo	0.209	0.054	0.091	<b>0.607</b>	0.039
Can Llobateres 1	0.062	0.005	<b>0.629</b>	0.304	0.001
Typicality probabilities					
Aberdares	0.081	0.015	0.087	<b>0.429</b>	0.003
Elgon	0.547	0.497	0.286	<b>0.675</b>	0.302
Kakamega	0.094	0.011	0.160	<b>0.340</b>	0.001
Masaii Mara	0.209	0.049	0.147	<b>0.579</b>	0.028
Mt Kenya	0.123	0.025	0.129	<b>0.575</b>	0.010
Nairobi	0.029	0.015	0.010	<b>0.048</b>	0.024
Naivasha	0.064	0.066	0.012	0.074	<b>0.111</b>
Shompole	0.414	0.028	0.717	<b>0.912</b>	0.005
Tsavo	0.230	0.080	0.122	<b>0.482</b>	0.062
Can Llobateres 1	0.100	0.013	<b>0.534</b>	0.333	0.002

<sup>a</sup> The highest probabilities for each locality are bolded.

localities of the Vallès-Penedès Basin in the future.

For the purposes of this work, estimates of paleotemperature (especially MAT) and paleoprecipitation (MAP) will be mainly discussed here. Neither MAT nor MAP estimates appear particularly accurate, with  $r^2 = 0.57$  and  $0.68$ , and  $r^{2*} = -0.05$  and  $0.38$ , respectively. Based on the equations’ accuracy, the paleoprecipitation estimate would be a priori more reliable, but this is uncertain because Zliobaité et al. (2016) provided no method for computing the confidence intervals of such estimates. In any event, the biome classification based on the paleotemperature (MAT) and paleoprecipitation (MAP) estimates for

CLL1 should be contrasted with other sources of evidence, such as those derived from stable isotope composition of mammalian tooth enamel (e.g., Koch, 1998; Kohn et al., 1998; Domingo et al., 2013; Higgins, 2018). These analyses are currently underway, but only preliminary results have been published so far (see below for further details). In the meantime, an alternative approach based on a multivariate analysis of FCT average values was undertaken to contrast the biome classification for CLL1 with that discussed earlier, based on the regression equations.

Based on the estimated values for paleotemperature (25 °C) and paleoprecipitation (881 mm), CLL1 would correspond to a tropical

**Table 8**

Whittaker's biome classification of Can Llobateres 1 and nine extant localities from Kenyan national parks (Žliobaitė et al., 2016) based on temperature and precipitation and a CVA of functional crown type variables.<sup>a</sup>

Locality	Whittaker's biome (TP)	Whittaker's biome (CVA)
Aberdares	Temperate seasonal forest	Tropical seasonal forest/savanna
Elgon	Temperate seasonal forest	Tropical seasonal forest/savanna
Kakamega	Temperate seasonal forest	Tropical seasonal forest/savanna
Masaai Mara	<b>Tropical seasonal forest/savanna</b>	<b>Tropical seasonal forest/savanna</b>
Mt Kenya	Temperate seasonal forest	Tropical seasonal forest/savanna
Nairobi	<b>Tropical seasonal forest/savanna</b>	<b>Tropical seasonal forest/savanna</b>
Naivasha	<b>Woodland/shrubland</b>	<b>Woodland/shrubland</b>
Shompole	<b>Tropical seasonal forest/savanna</b>	<b>Tropical seasonal forest/savanna</b>
Tsavo	<b>Tropical seasonal forest/savanna</b>	<b>Tropical seasonal forest/savanna</b>
Can Llobateres 1	Tropical seasonal forest/savanna	Tropical rainforest

Abbreviations: TP = temperature and precipitation; CVA = canonical variate analysis.

<sup>a</sup> Biome names are bolded for those localities in which both methods yield the same biome attributions.

seasonal forest/savanna according to Whittaker's biome scheme. The biome classification based on the CVA is not entirely coincident as CLL1 is classified as a tropical rainforest with a posterior probability of 63%. Such a discrepancy is not surprising as the CVA is based on the seven FCT variables, whereas the paleotemperature and paleoprecipitation estimates are calculated from different subsets of three variables each, overall including only four out of the seven FCT variables. Furthermore, the classification accuracy of the CVA is moderately low (49.5%). Given all these caveats, it is remarkable that the biome classification based on paleoenvironmental estimates (tropical seasonal forest/savanna) coincides with the second most-likely classification of the CVA, with a posterior probability of 30%. From a purely statistical viewpoint, CLL1 falls in an area of the ecomorphospace where the 95% confidence ellipses of both biomes overlap, with the tropical rainforest biome displaying a much more restricted scatter than tropical seasonal forest/savanna. Moreover, extant localities from the tropical seasonal forest/savanna biome are as frequently misclassified as tropical rainforest as correctly classified (42% in both cases), whereas tropical rainforest localities are most frequently classified correctly and are only seldom misclassified as tropical seasonal forest/savanna. Therefore, it seems logical to conclude that CLL1 most likely belongs to the tropical seasonal forest/savanna biome. Alternatively, CLL1 might belong to a tropical rainforest biome, which differs from the tropical seasonal forest/savanna biome by displaying much higher precipitation values. This would imply that the annual precipitation estimate derived for CLL1 largely underestimates the actual value, which must be more than twice the estimate (>2500 mm instead of 881 mm at 25 °C, based on

Whittaker's scheme). This seems unlikely even if paleotemperature is overestimated, but not completely impossible, given the low accuracy of the paleoprecipitation regression equation. A third possible explanation, not mutually exclusive with the first one, is that CLL1 records a mosaic of habitats that, despite falling within the tropical seasonal forest/savanna biome, mimics the faunal composition that would be expected in a tropical rainforest habitat—owing to local paleoenvironmental conditions favoring the presence of taxa adapted to more humid environments. These possibilities are evaluated in the next subsection, based on the fossil flora and fauna from CLL1, as well as in relation to preliminary data on tooth enamel isotopic data.

Whittaker's biome classification is one of the simplest schemes to distinguish terrestrial biomes as it only considers MAT and MAP. While the scheme is calibrated on the present day and, in all probability, does not identically apply to the deep past, it can be applied to the Miocene to a first approximation. Other biome classification systems, such as Walter (1979), consider seasonality in both temperature and precipitation. Since the methods used allow inferring which are the coldest/warmest and wettest/driest months in the studied localities, these biome classification schemes can be considered as well. The MAT is above 20 °C, which indicates a tropical climate (according to Köppen–Geiger climate classification; see Peel et al., 2007) with little temperature seasonality since it ranges from 24.4 °C in the coldest month to 26.7 °C in the warmest. The MAP is also high (881 mm) for a tropical environment such as savanna or desert with average monthly precipitation always being above 100 mm. However, the inferred rainfall seasonality is remarkable, with precipitation in the wettest month (2119 mm) being

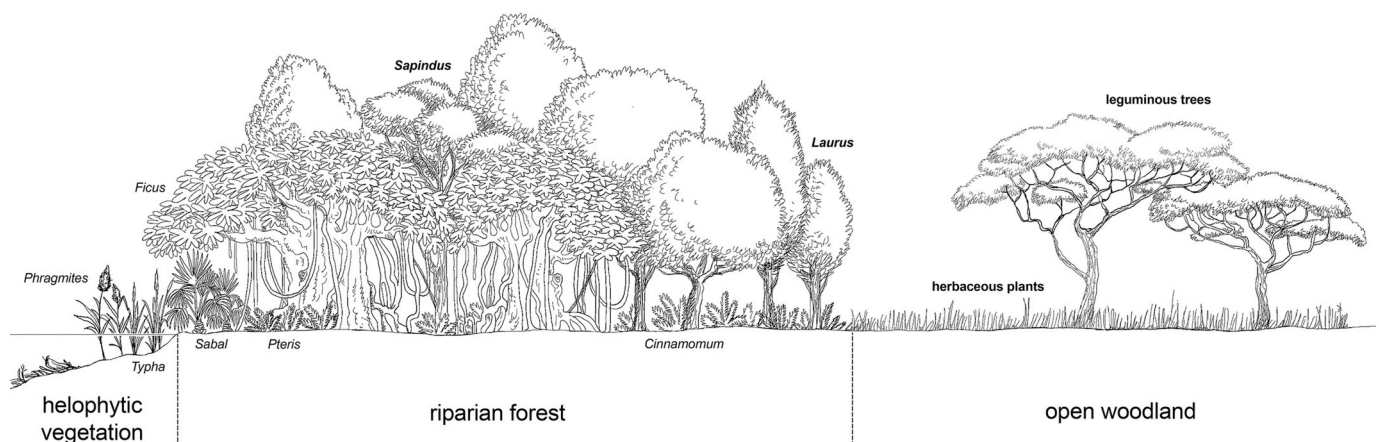


**Figure 5.** Schematic vegetation profile for Can Llobateres 1 based on macrofloral remains recovered from the site. Vegetation zones as well as names of characteristic plants are also indicated. Bold font indicates taxa that have not been recovered at Can Llobateres 1 but occur in other sites of the same basin. A marshy environment populated by reeds (*Phragmites* and *Typha*) is depicted to the left, bordered by a dense riparian evergreen forest with palms (*Sabal*), figs (*Ficus*), and laurels (*Cinnamomum*) that would have represented a favorable habitat for hominoids. A more arid, open, and seasonal environment, including areas dominated by leguminous trees, shrubs, and herbaceous plants, is depicted to the right far from the wetlands. Artwork by Roc Olivé.

more than 10-times higher than that recorded during the driest month (136 mm). Such precipitation seasonality is consistent with a tropical seasonal biome, with a clear rainy season. Nonetheless, there is a gradient between evergreen tropical forests and tropical deciduous forests depending on the length and severity of the dry season, with tropical seasonal forests (also called semievergreen or mixed tropical forests), corresponding to zonoecotone I/II of [Walter \(1979\)](#), showing an intermediate composition, characterized by the presence of some deciduous tree species that lose their leaves during the dry season. Vegetation structure in tropical seasonal forests includes different canopy layers as in rainforests, but generally stratification is less complex, the canopy is relatively more open, epiphytes and especially lianas are abundant, and ground vegetation is more diverse and abundant (see [Walter, 1979](#); [Allaby, 2006](#)). In a tropical seasonal biome, the driest month typically records less than 60 mm of rainfall, which is much lower than the values inferred for CLL1, suggesting that the latter might have been characterized by a tropical seasonal forest somewhat intermediate between a tropical evergreen and a tropical deciduous forest.

**Comparison with previous paleoenvironmental inferences for Can Llobateres 1** The summary of previous paleoenvironmental inferences for CLL1 provided in [Table 1](#) highlights some similar conclusions among authors but also some discrepancies regarding the openness of the habitat and the seasonality of the climate. [Nagatoshi \(1987\)](#) concluded that most of the primate-bearing sites of the Middle and Late Miocene of western Eurasia were characterized by the presence of water and interpreted CLL1 as an open environment with some intruding marshy areas, based on the presence of *Hippotherium* and *Tapirus*. However, the paleobotanical evidence is rather suggestive of a closed forest next to a marshy area with more open environments at some distance ([Fig. 5](#); [Marmi et al., 2012](#)). The fossil plant assemblage from CLL1 ([Álvarez Ramis, 1975](#); [Sanz de Siria Catalán, 1993, 1994](#); [Marmi et al., 2012](#)) is composed of abundant reed remains (*Phragmites* and *Typha*), coupled with palms, evergreen laurels, and fig trees (*Ficus* sp.). The reeds are suggestive of a marshy area, whereas the rest of the vegetation denotes the nearby presence of a dense wetland or a riparian forest ([Alba et al., 2011a, 2011b](#); [Marmi et al., 2012](#); [Andrews, 2015](#)). In turn, the presence of mega-mesothermal taxa and the absence of deciduous taxa indicate a subtropical to warm-temperate climate characterized by high MATs ([Marmi et al., 2012](#)). [Sanz de Siria Catalán \(1994\)](#) inferred subtropical conditions based on the then-available flora from CLL1. Although such inferences must be taken with care, given that CLL1 corresponds to an azonal plant community, they are consistent with the estimated MAT of 26 °C derived in this work from FCT variables. According to the Köppen–Geiger climate classification (updated by [Peel et al., 2007](#)), a tropical climate is characterized by average temperatures above 18 °C in the coldest month, whereas a subtropical (or temperate) climate displays average temperatures above 10 °C in the hottest month and between 0 and 18 °C in the coldest month. Therefore, the paleotemperature estimates for CLL1 based on FCT variables for the hottest month (26.7 °C) and the coldest month (24.4 °C) indicate a tropical climate, consistent with the two biome attributions favored by the analyses. On the other hand, paleobotanical evidence from other localities and nearby basins suggests that the plant community from CLL1 would not be representative of the zonal vegetation, which would have been characterized by a higher proportion of mega-mesothermal taxa and deciduous elements, overall denoting subtropical to warm-temperate (rather than tropical) climate conditions in the Vallès-Penedès Basin around the transition between the early and late Vallesian ([Marmi et al., 2012](#), and references therein). It is thus reasonable to assume that, far from the wetlands, more open woodlands would have been present by this time ([Alba et al., 2011a, 2011b](#); [Marmi et al., 2012](#)) and that paleotemperature estimates for CLL1 based on FCT variables might be biased to some extent toward higher temperatures than were actually present in the area by that time.

As stressed by [Marmi et al. \(2012\)](#) and [Andrews \(2015\)](#), the faunal composition of CLL1 further supports the presence of a marshy depositional environment, given the presence of beavers ([Marmi et al., 2012](#);

[Andrews, 2015](#)), the bovid *M. pannoniae* (which displays adaptations to wet environments; [Köhler, 1993](#)), and the tragulid *D. navi* (which shows many similarities with the extant water chevrotian, a forest-dwelling frugivorous animal with aquaphilous preferences; [Alba et al., 2011c](#), and references therein). The presence of large browsing herbivores (*C. goldfussi*, *M. aff. flourensianus*, *A. anocerus*, *T. priscus*, cf. *Ac. incisivum*, and *Alicornops simorreense*), in turn, is indicative of a densely forested environment ([Marmi et al., 2012](#)), which is further supported by a diverse assemblage of flying squirrels and tree dormice, which are quite diverse, albeit not particularly abundant ([Casanovas-Vilar and Agustí, 2007](#); [Marmi et al., 2012](#); [Casanovas-Vilar et al., 2015](#)). Flying squirrels are remarkably diverse, including up to five different species representing both large (*Miopetaurista crusafonti*, *Miopetaurista neogrivensis*, *Albanensia* aff. *grimmii*) and small (*Blackia miocaenica*, cf. *Pliopetaurista* sp.) species. Such diversity of flying squirrels is currently only recorded in the tropical and subtropical forests of southeastern Asia, which show a complex and stratified canopy ([Jackson, 2012](#); [Lu et al., 2013](#)). This is further consistent with the presence of a large-bodied ape such as *H. laietanus*, particularly given the previous locomotor inferences based on its partial skeleton, indicating that it possessed an orthograde body plan with suspensory adaptations, even if displaying a higher degree of above-branch quadrupedalism than extant apes ([Moyà-Solà and Köhler, 1996](#); [Almécija et al., 2007](#); [Alba et al., 2010, 2012b](#); [Pina et al., 2012](#); [Tallman et al., 2013](#); [Susanna et al., 2014](#)). On the other hand, the presence of a giraffid ([Köhler, 1993](#)) and rodents such as the cricetid *Hispanomys* and ground squirrels ([Casanovas-Vilar and Agustí, 2007](#)) hint at the presence of more open woodlands nearby ([Marmi et al., 2012](#)).

Unlike other artiodactyls, suids have not been previously considered when making paleoenvironmental inferences for CLL1, even though they can provide interesting insights. The taxonomic revision of the large herbivorous mammals from CLL1 performed in this work has confirmed the presence of a diverse suid assemblage, clearly dominated by the small tetraconodontine *Pa. crusafonti* but further including (in order of decreasing abundance) *P. palaeochoerus*, *L. splendens*, and *Pa. valentini*. The dietary ecology of *L. splendens* has been thoroughly discussed as these suids stand out by its lophodont morphology and the lack of adaptations for the rooting feeding behaviors characteristic of most suids ([Fortelius et al., 1996a](#); [Van der Made et al., 2014, 2022](#)), allowing them to survive when other types of food are scarce. The occlusal morphology of *L. splendens* was originally interpreted as an adaptation for a mainly folivorous diet ([Van der Made, 1996](#)) and microwear analyses supported that this species was mainly a browser ([Hunter and Fortelius, 1994](#)). This has been confirmed by isotopic analyses, which further suggest a considerable consumption of fruits and maybe some grass ([Aiglstorfer et al., 2014](#)). [Van der Made et al. \(2014\)](#) hypothesized that *L. splendens* would have inhabited relatively open or mosaic environments, but most recently, [Van der Made et al. \(2022\)](#) favored the view that, given the lack of rooting adaptations, *Listriodon* would have been more limited than other suids to environments where nutritious leaves and fruits were available throughout the year. Based on dental morphology, it has been inferred that *P. palaeochoerus* would have been even better adapted for rooting behaviors than medium to large-sized tetraconodontines of the genera *Parachleuastochoerus* and *Versoporcus* ([Van der Made, 2010](#); [Van der Made et al., 2014](#)). However, isotopic data indicate that these tetraconodontines also consumed underground resources ([Aiglstorfer et al., 2014](#)), and indeed isotopic data and trace elements from Rudabánya (Hungary)—a hominoid-bearing site roughly coeval to CLL1—indicate that tetraconodontines might have fed on such resources more frequently than *Propotamochoerus* ([Eastham et al., 2016, 2017](#); [Iannucci and Begun, 2022](#)). This suggests a more varied omnivorous diet for *Propotamochoerus*, in agreement with the greater development of secondary cusps typical of suines ([Fortelius et al., 1996a](#)).

These dietary inferences for suids recorded at CLL1 are relevant for interpreting the extinction of *H. laietanus* because some parallelism can be established with the diet of *H. laietanus* and also because the

extinction of *L. splendens* has been related to the paleoenvironmental changes during the early/late Vallesian transition, which are generally considered the trigger of the Vallesian Crisis (Van der Made et al., 2022). The latter is a regional turnover event, originally identified in the Vallès-Penedès Basin, that allegedly implied the extinction of mammals adapted to warm and humid forested environments and their replacement by taxa adapted to more open and drier environments (Agustí and Moyà-Solà, 1990; Moyà-Solà and Agustí, 1990). The extension of the Vallesian Crisis to a continental scale (e.g., Fortelius et al., 1996b; Agustí et al., 1999) has been questioned (Casanovas-Vilar et al., 2005, 2010), being alternatively attributable to sampling biases (Casanovas-Vilar et al., 2014, 2016a). This has been conclusively shown based on micromammals from the Vallès-Penedès Basin (Casanovas-Vilar et al., 2014), where the correction of such biases indicates that the purported Vallesian Crisis was a protracted faunal turnover rather than an abrupt extinction event. Although this remains to be ascertained for large mammals, it has been convincingly argued that changes in vegetation structure led to the extinction of multiple forest-adapted frugivorous taxa, particularly primates (Agustí et al., 2003; Marmi et al., 2012; Casanovas-Vilar et al., 2016a) and some suids (Van der Made et al., 2022).

Dental microwear analyses indicate that *H. laietanus* displayed a frugivorous diet (Ungar, 1996; DeMiguel et al., 2014), probably emphasizing soft ripe fruits but also including hard fruits as fallback fruits on a seasonal basis (DeMiguel et al., 2014). This would have allowed this species to survive in the face of marked environmental instability around the early/late Vallesian transition. This is supported by the presence of abundant enamel hypoplasias (Skinner et al., 1995; Eastham et al., 2009), which indicate repeated episodes of malnutrition due to seasonal resource abundance fluctuations, suggesting that *H. laietanus* probably feed on hard foods during the unfavorable season (DeMiguel et al., 2014). Although there are no paleodietary data for *Pa. crusafonti*, small suids are generally interpreted as forest-adapted forms (Fortelius et al., 1996a), in agreement with the abundance in this taxon at CLL1. This suggests that *Pa. crusafonti* might have displayed on the ground a similar feeding strategy to that of *H. laietanus* in an arboreal niche, i.e., predominantly based on fruits and recouring to other resources during the most unfavorable months of the year (maybe thanks to rooting behaviors). The moderately abundant *P. palaeochoerus*, like the scarce *Pa. valentini*, could have exploited other trophic resources and preferentially inhabited the more open areas far from the wetland. In contrast, this explanation is more unclear in the case of *L. splendens*, whose scarcity at CLL1 might be related to the lack of a continuous fruit supply during the unfavorable season, given its lack of rooting adaptations.

With regard to the biome classification of CLL1 as a tropical rainforest or a tropical seasonal forest/savanna biome, it is worth comparing it with the results obtained by previous authors using different methods. The analyses of mammalian community structure performed by Andrews (1996) using different methods reconstructed both CLL1 and Rudabánya as subtropical seasonal forests, thus supporting a classification of the former as a tropical seasonal forest rather than as a tropical rainforest (note that an alternate classification of CLL1 as a temperate rain or seasonal forest biome is discounted by the results of our analyses). Similarly, based on multivariate analyses of faunal composition, Hernández Fernández et al. (2003) classified CLL1 as a deciduous tropical forest with a posterior probability of 99.5%—the second option (savanna) and other remaining possibilities (rainforest and laurel forest) being very unlikely. Despite being based on a much less sophisticated approach, the results of Hernández Fernández et al. (2003) are also broadly consistent with those derived in this work, supporting that CLL1 is more readily interpreted as a tropical seasonal forest/savanna biome than as a tropical rainforest. By contrast, Costeur's (2005) cenogram analyses concluded that CLL1 displayed more closed and humid conditions than Rudabánya, attributing the former to a tropical forest and the latter to a subtropical forest/savanna mosaic. Additional support to the

classification of CLL1 as a tropical seasonal forest/savanna instead of a tropical rainforest comes from preliminary isotope analyses performed on muroid rodents from the Vallès-Penedès Basin (Casanovas-Vilar et al., 2019, 2020). These confirm that hominoid-bearing sites are more humid on average than those where primates are not recorded, with most of the former being in the range of tropical deciduous forests to evergreen warm mixed forests. For CLL1, paleoprecipitation estimates derived from muroid stable isotopes result in MAP well above 1000 mm, while the paleotemperature estimate is comparable to that derived in this work (I.C.V., unpublished data). Nevertheless, the value derived from isotopes is much lower than the one that would be expected for a tropical rainforest, confirming that CLL1 does not correspond to this type of biome. Unpublished isotope analyses based on the equid *Hip. catalaunicum* from CLL1 indicate a diet entirely based on C<sub>3</sub> vegetation (Misas Alcántara, 2022). Following the methods by Kohn (2010), these can be used to infer paleoprecipitation, although ideally a broader taxonomic sample should be considered for the calculations. Tooth enamel  $\delta^{13}\text{C}$  ranges from  $-10.7\text{‰}$  to  $-12.5\text{‰}$  (Misas Alcántara, 2022), which results in a MAP estimation of  $\sim 700\text{--}1000$  mm, thus consistent with the results yielded by the multivariate analyses of FCT variables. Misas Alcántara (2022) noted that, if *Hip. catalaunicum* had inhabited and fed in the locally humid environment next to the depositional environment, this would have resulted in more negative isotopic values—in further agreement with the greater abundance of *Hippotherium* remains in the channel deposits than in the primate-bearing levels of CLL1. Therefore, the values reported are taken as an indication of less humid, and presumably more open, environments nearby.

It has been hypothesized that *H. laietanus* would have preferred the humid forested environments close to permanent water due to the availability of ripe, soft fruit supplies on a year-round basis (Alba et al., 2011a, 2011b; Marmi et al., 2012), or at least during part of the year (DeMiguel et al., 2014), despite the fact that warm-temperate mixed forests, composed mainly of deciduous taxa, would have probably been present far from these wetlands (Alba et al., 2011a, 2011b; Marmi et al., 2012). Similarly, the roughly coeval *Rudapithecus hungaricus* from Rudabánya (Hungary) is associated with a subtropical swamp forest dominated by swamp cypress (*Taxodium*; Andrews and Cameron, 2010; Andrews, 2015). Tooth enamel stable isotope analyses of the large mammal assemblage of Rudabánya indicate a mosaic of environments and ecological niche partitioning (Eastham et al., 2016). Some taxa, such as *D. nauii* and *C. goldfussi*, would have fed in closed canopy environments, whereas others such as *Hippotherium intrans* would have preferred more open habitats. Therefore, the environment associated with *R. hungaricus* in Rudabánya has strong similarities with that associated with *H. laietanus* in CLL1, the two corresponding to local wetlands. However, there are also some differences because the riparian forest composition (as evidenced from paleobotanical data) is clearly different and woodlands away from the wetlands appear to have been more humid and warm-temperate in Rudabánya (Andrews, 2015).

Within such environments, Late Miocene dryopithecines occupied a mainly arboreal and frugivorous niche. Although these environments might have been quite common in the Vallès-Penedès Basin during the early Vallesian (Alba et al., 2011b; Marmi et al., 2012), from the late Vallesian onward, tropical and subtropical taxa (such as palm and fig trees) would have progressively disappeared as temperatures dropped (Sanz de Siria Catalán, 1994), while deciduous trees (such as poplars or willows) became dominant in forested areas and wetlands (Agustí et al., 2003; Alba et al., 2011a, 2011b; Marmi et al., 2012). As a result, these new environments would not have provided the necessary resources to sustain a population of *H. laietanus* (and other taxa dependent on forest trophic resources, such as probably *Pa. crusafonti* and *L. splendens*) throughout the year, especially during the cold season, leading to their progressive demise and eventual extinction in the Vallès-Penedès Basin and other areas of Western Europe (Agustí et al., 2003; Casanovas-Vilar et al., 2005, 2010; Alba et al., 2011a, 2011b; Marmi et al., 2012). In this regard, it is noteworthy that the record of *L. splendens* from CLL1

represents the latest well-dated occurrence of this taxon in Europe, whereas *Pa. crusafonti* is last recorded slightly later at La Tarumba 1 (Van der Made, 1990, 1997; Van der Made et al., 2022) at ~9.6 Ma (Casanovas-Vilar et al., 2016b), coinciding with the last record of *H. laietanus* (Casanovas-Vilar et al., 2011; Alba et al., 2018). The extinction of hominoids in other areas of Western mainland Europe would have followed a similar, although diachronous, pattern (Agustí et al., 2003; Merceron et al., 2010; Casanovas-Vilar et al., 2010, 2011; DeMiguel et al., 2014).

## 5. Conclusions

This study for the first time applied a full FCT scheme to analyze a Miocene fossil site. The results of this work indicate that FCT variables in combination with regional predictive models calibrated on Kenyan national parks as well as case-based reasoning over a selection of present-day biomes are not very powerful for providing unambiguous biome classifications for CLL1. Paleoprecipitation values appear potentially more biased than paleotemperature estimates, which show a greater agreement with isotopic data and both plant and faunal composition. CVAs, in turn, failed to distinguish some particular biomes. Nevertheless, when both approaches based on FCT variables are combined, the results are in broad agreement with previous inferences based on other sources of data, suggesting that FCT variables are a useful complementary approach to make ecometric comparisons among multiple sites with limited associated cost, thus being potentially useful to refine inferences based on other, more traditional methods of paleoecological inference.

Regarding CLL1, the multivariate analyses based on FCT support a biome classification as tropical rainforest or tropical seasonal forest/savanna, but paleotemperature and paleoprecipitation estimates, particularly considering the amplitude of rainfall seasonality, are in better agreement with the latter. These results are in further accordance with previous inferences derived from fossil plants and mammals, as well as preliminary isotopic data. Based on these other sources of evidence, it is concluded that the inability of the multivariate analysis to unambiguously classify CLL1 as a tropical seasonal forest is due to the fact that the fossil assemblage mixes forest-adapted taxa (such as *H. laietanus* and *Pa. crusafonti*), likely restricted to the closed forest environment surrounding the marshy depositional area, with other taxa that likely inhabited more open woodland environments far from the wetland (such as *Propotamochoerus* and *Hippotherium*). In other words, the CLL1 local paleoenvironment to which *H. laietanus* was adapted, in isolation, would not be representative of the biome at a more regional scale, characterized by a mosaic of dense forests around the wetlands and more open vegetation between these areas. Overall, our results are consistent with previous studies that related the extinction of frugivorous hominoids in Western mainland Europe with that of other forest-adapted taxa—the so-called Vallesian Crisis. Even though paleobiodiversity analyses of micromammals suggest that this was a more protracted event rather than an abrupt crisis, it remains to be determined if the same applies to large mammals, or whether some important paleoenvironmental threshold (such as the complete replacement of tropical seasonal forest patches by deciduous tropical forests) was surpassed at ~9.5 Ma, at least in the Vallès-Penedès Basin. Future studies based on FCT variables in other well-sampled Vallesian localities of this basin, preceding (e.g., Castell de Barberà, Creu de Conill, Can Poncic) or postdating (e.g., La Tarumba, Torrent de Febulines) CLL1, might provide further precision in assessing the causes of the extinction of Miocene apes in Europe.

## Conflict of interest

The authors declare no competing interests.

## Acknowledgments

This article is part of R+D+I projects PID2020-117289GB-I00, PID2020-116908GB-I00, and PID2020-116220GB-I00, funded by the Agencia Estatal de Investigación of the Spanish Ministerio de Ciencia e Innovación (MCIN/AEI/10.13039/501100011033/) and has also been supported by the Agència de Gestió d'Ajuts Universitaris i de Recerca of the Generalitat de Catalunya (2001 SGR 00620) and the Generalitat de Catalunya/CERCA Programme, and the Government of Aragón (Research Group ref. E33\_23R). S.G.A. enjoys a technician contract of the INVESTIGO Program 2022 (reference 100027TC1) financed by the European Union, Next Generation EU. I.Ž. acknowledges research funding by the Academy of Finland (grant no. 341623). O.C. gratefully acknowledges funding to R.L.B. (NSF ABI 1759882) and Howard University, for his support as a postdoctoral research fellow at Howard University, Washington D.C. We are grateful to Alessandro Urciuoli, Florian Bouchet, and Oriol Monclús-Gonzalo for statistical advice, as well as Salvador Moyà-Solà and Víctor Vinuesa for discussion about fossil material. This work is part of the Ph.D. Dissertation of the first author, in the framework of the Ph.D. Programme in Biodiversity of the Universitat Autònoma de Barcelona. Finally, we thank the Editor (Clément Zanolli), the Associate Editor, and three anonymous reviewers for helpful and constructive comments that helped us improve a previous draft of this paper.

## Supplementary Online Material

Supplementary Online Material to this article can be found online at <https://doi.org/10.1016/j.jhevol.2023.103441>.

## References

- Agustí, J., Moyà-Solà, S., 1990. Mammal extinctions in the Vallesian (Upper Miocene). *Lect. Notes Earth Sci.* 30, 425–432.
- Agustí, J., Köhler, M., Moyà-Solà, S., Cabrera, L., Garcés, M., Parés, J.M., 1996. Can Llobateres: The pattern and timing of the Vallesian hominoid radiation. *J. Hum. Evol.* 31, 143–155.
- Agustí, J., Cabrera, L., Garcés, M., Parés, J.M., 1997. The Vallesian mammal succession in the Vallès-Penedès basin (northeast Spain): Paleomagnetic calibration and correlation with global events. *Palaeogeogr. Palaeoclimatol. Palaeoecol.* 133, 149–180.
- Agustí, J., Cabrera, L., Garcés, M., Llenas, M., 1999. Mammal turnover and global climate change in the late Miocene terrestrial record of the Vallès-Penedès basin (NE Spain). In: Agustí, J., Rook, L., Andrews, P. (Eds.), *The Evolution of Neogene Terrestrial Ecosystems in Europe*. Cambridge University Press, Cambridge, pp. 397–411.
- Agustí, J., Sanz de Siria Catalán, A., Garcés, M., 2003. Explaining the end of the hominoid experiment in Europe. *J. Hum. Evol.* 45, 145–153.
- Aiglstorfer, M., Bocherens, H., Böhme, M., 2014. Large mammal ecology in the late Middle Miocene Gratkorn locality (Austria). *Palaeobiodiv. Palaeoenviron.* 94, 189–213.
- Alba, D.M., 2012. Fossil apes from the Vallès-Penedès Basin. *Evol. Anthropol.* 21, 254–269.
- Alba, D.M., Almécija, S., Moyà-Solà, S., 2010. Locomotor inferences in *Pierolapithecus* and *Hispanopithecus*: Reply to Deane and Begun (2008). *J. Hum. Evol.* 59, 143–149.
- Alba, D.M., Casanovas-Vilar, I., Moyà-Solà, S., Robles, J.M., 2011a. Parada 4. El Vallesiense Inferior y su transición con el Vallesiense Superior. *Can Llobateres. Paleontol. Evol. Mem. Espec.* 6, 111–123.
- Alba, D.M., Casanovas-Vilar, I., Robles, J.M., Marmi, J., Moyà-Solà, S., 2011b. New paleontological excavations at the Late Miocene site of Can Llobateres 1 (Vallès-Penedès Basin, NE Iberian Peninsula): Preliminary results of the 2010 campaign. In: Pérez-García, A., Gascó, F., Gasulla, J.M., Escaso, F. (Eds.), *Viajando a Mundos Pretéritos. Ayuntamiento de Morella, Morella*, pp. 35–43.
- Alba, D.M., Moyà-Solà, S., Robles, J.M., Casanovas-Vilar, I., Rotgers, C., Carmona, R., Galindo, J., 2011c. Middle Miocene tragusid remains from Abocador de Can Mata: The earliest record of *Dorcatherium nauti* from Western Europe. *Geobios* 44, 135–150.
- Alba, D.M., Casanovas-Vilar, I., Almécija, S., Robles, J.M., Arias-Martorell, J., Moyà-Solà, S., 2012a. New dental remains of *Hispanopithecus laietanus* (Primates: Hominidae) from Can Llobateres 1 and the taxonomy of Late Miocene hominoids from the Vallès-Penedès Basin (NE Iberian Peninsula). *J. Hum. Evol.* 63, 231–246.
- Alba, D.M., Almécija, S., Casanovas-Vilar, I., Méndez, J.M., Moyà-Solà, S., 2012b. A partial skeleton of the fossil great ape *Hispanopithecus laietanus* from Can Feu and the mosaic evolution of crown-hominoid positional behaviors. *PLoS One* 7, e39617.
- Alba, D.M., Casanovas-Vilar, I., Furió, M., García-Paredes, I., Angelone, C., Jovells-Vaqué, S., Luján, Á.H., Almécija, S., Moyà-Solà, S., 2018. Can Pallars i Llobateres: A new hominoid-bearing locality from the late Miocene of the Vallès-Penedès Basin (NE Iberian Peninsula). *J. Hum. Evol.* 121, 193–203.

- Alba, D.M., Gasamans, N., Pons-Monjo, G., Luján, À.H., Robles, J.M., Obradó, P., Casanovas-Vilar, I., 2020. Oldest *Deinotherium proavum* from Europe. *J. Vertebr. Paleontol.* 40, e1775624.
- Alba, D.M., Torres, J., DeMiguel, D., Casanovas-Vilar, I., 2022a. The Vallès-Penedès Miocene Vertebrates Paleobiodiversity Database. In: Casanovas-Vilar I., Alba D.M. (Eds.), NOW 25th Anniversary Meeting. Sabadell (Barcelona), 16–18 November 2022. Abstract Book & Fieldtrip Guide. *Paleontol. Evol. Mem. Espec.* 9, 59–60.
- Alba, D.M., Robles, J.M., Casanovas-Vilar, I., Beamud, E., Bernor, R.L., Cirilli, O., DeMiguel, D., Galindo, J., Llopart, I., Pons-Monjo, G., Sánchez, I.M., Vinuesa, V., Garcés, M., 2022b. A revised (earliest Vallesian) age for the hominoid-bearing locality of Can Mata 1 based on new magnetostratigraphic and biostratigraphic data from Abocador de Can Mata (Vallès-Penedès Basin, NE Iberian Peninsula). *J. Hum. Evol.* 170, 103237.
- Alberdi, M.T., 1974. El género *Hipparion* en España. Nuevas formas de Castilla y Andalucía, revisión e historia evolutiva. In: *Trabajos sobre Neógeno-Cuaternario 1*. Instituto Lucas Mallada, C.S.I.C., Madrid, pp. 1–219.
- Allaby, M., 2006. *Biomes of the Earth: Tropical forests*. Chelsea House Publishers, New York.
- Almécija, S., Alba, D.M., Moyà-Solà, S., Köhler, M., 2007. Orang-like manual adaptations in the fossil hominoid *Hispanopithecus laietanus*: First steps towards great ape suspensory behaviours. *Proc. R. Soc. B* 274, 2375–2384.
- Almécija, S., Hammond, A.S., Thompson, N.E., Pugh, K.D., Moyà-Solà, S., Alba, D.M., 2021. Fossil apes and human evolution. *Science* 372, eabb4363.
- Álvarez Ramis, C., 1975. Quelques considérations écologiques sur le gisement Vallésien de Can Llobateres (Barcelona, Espagne). In: *Comptes Rendus du 100e Congrès National des Sociétés Savantes (Paris, 1975)*. Fascicule II. Bibliothèque Nationale, Paris, pp. 11–16.
- Andrews, P., 1996. Palaeoecology and hominoid palaeoenvironments. *Biol. Rev.* 71, 257–300.
- Andrews, P., 2015. *An Ape's View of Human Evolution*. Cambridge University Press, Cambridge.
- Andrews, P., Cameron, D., 2010. Rudabánya: Taphonomic analysis of a fossil hominid site from Hungary. *Paleoecogr. Palaeoclimatol. Palaeoecol.* 297, 311–329.
- Anquetin, J., Antoine, P.O., Tassy, P., 2007. Middle Miocene Chalicotheriinae (Mammalia, Perissodactyla) from France, with a discussion on chalicotheriine phylogeny. *Zool. J. Linn. Soc.* 151, 577–608.
- Azanza, B., Menéndez, E., 1990. Los ciervos fósiles del neógeno español. *Paleontol. Evol.* 23, 75–82.
- Begun, D.R., 1994. Relations among the great apes and humans: New interpretations based on the fossil great ape *Dryopithecus*. *Yearb. of Phys. Anthropol.* 19, 11–63.
- Begun, D.R., 2009. *Dryopithecines*, Darwin, de Bonis, and the European origin of the African apes and human clade. *Geodiversitas* 31, 789–816.
- Begun, D.R., Moyà-Solà, S., Köhler, M., 1990. New Miocene hominoid specimens from Can Llobateres (Vallès Penedès, Spain) and their geological and paleoecological context. *J. Hum. Evol.* 19, 255–268.
- Bergounioux, F.M., Crouzel, F., 1962. Les Deinotheridés d'Espagne. *Bull. Soc. Geol. Fr.* 4, 394–404.
- Bernor, R.L., Woodburne, M.O., Van Couvering, J.A., 1980. A contribution to the chronology of some Old World Miocene faunas based on hipparionine horses. *Geobios* 13, 705–739.
- Bernor, R.L., Koufos, G.D., Woodburne, M.O., Fortelius, M., 1996. The evolutionary history and biochronology of European and Southwest Asian Late Miocene and Pliocene Hipparionine horses. In: Bernor, R.L., Fahlbusch, V., Mittmann, H.-W. (Eds.), *The Evolution of Western Eurasian Neogene Faunas*. Columbia University Press, New York, pp. 307–338.
- Bernor, R.L., Tobien, H., Hayek, L.-A.C., Mittmann, H.-W., 1997. *Hippotherium primigenium* (Equidae, Mammalia) from the late Miocene of Höwenegg (Hegau, Germany). *Andrias* 10, 5–230.
- Bernor, R.L., Kaya, F., Kaakinen, A., Saarinen, J., Fortelius, M., 2021. Old world hipparion evolution, biogeography, climatology and ecology. *Earth Sci. Rev.* 221, 103784.
- Bernor, R.L., Cirilli, O., Mittmann, H.-W., 2022. Höwenegg *Hippotherium primigenium*: Geological context, cranial and postcranial morphology, palaeoecological and biogeographic importance. *Hist. Biol.* 35, 1376–1390.
- Bougeard, S., Dray, S., 2018. Supervised multiblock analysis in R with the ade4 package. *J. Stat. Softw.* 86, 1–17.
- Cailleux, F., Van den Hoek Ostende, L.W., Joniak, P., in press. The Late Miocene Erinaceidae and Dimylidae (Eulipotyphla, Mammalia) from the Pannonian Region. *J. Paleontol.*
- Cameron, D.W., 1997. A revised systematic scheme for the Eurasian Miocene fossil Homiidae. *J. Hum. Evol.* 33, 449–477.
- Cameron, D.W., 1998. Patterns of facial sexual dimorphism in *Hispanopithecus*. *Z. Morphol. Anthropol.* 82, 47–58.
- Cameron, D.W., 1999. The single species hypothesis and *Hispanopithecus* fossils from the Vallès Penedès Basin, Spain. *Z. Morphol. Anthropol.* 82, 159–186.
- Cameron, D.W., 2004. *Hominid Adaptations and Extinctions*. University of New South Wales Press, Sydney.
- Casanovas-Vilar, I., Agustí, J., 2007. Ecogeographical stability and climate forcing in the Late Miocene (Vallesian) rodent record of Spain. *Paleoecogr. Palaeoclimatol. Palaeoecol.* 248, 169–189.
- Casanovas-Vilar, I., Moyà-Solà, S., Agustí, J., Köhler, M., 2005. The geography of a faunal turnover: Tracking the Vallesian Crisis. In: Elewa, A.T. (Ed.), *Migration of Organisms: Climate, Geography, Ecology*. Springer, Heidelberg, pp. 247–301.
- Casanovas-Vilar, I., García-Paredes, I., Alba, D.M., van den Hoek Ostende, L., Moyà-Solà, S., 2010. The European Far West: Miocene mammal isolation, diversity and turnover in the Iberian Peninsula. *J. Biogeogr.* 37, 1079–1093.
- Casanovas-Vilar, I., Alba, D.M., Garcés, M., Robles, J.M., Moyà-Solà, S., 2011. Updated chronology for the Miocene hominoid radiation in Western Eurasia. *Proc. Natl. Acad. Sci. USA* 108, 5554–5559.
- Casanovas-Vilar, I., Van den Hoek Ostende, L., Furió, M., Madern, P.A., 2014. The range and extent of the Vallesian Crisis (Late Miocene): New prospects based on the micromammal record from the Vallès-Penedès Basin (Catalonia, Spain). *J. Iber. Geol.* 40, 29–48.
- Casanovas-Vilar, I., Almécija, S., Alba, D.M., 2015. Late Miocene flying squirrels from Can Llobateres 1 (Vallès-Penedès Basin, Catalonia): Systematics and paleobiogeography. *Palaeobiodiversity Database*. 95, 353–372.
- Casanovas-Vilar, I., Madern, A., Alba, D.M., Cabrera, L., García-Paredes, I., Van den Hoek Ostende, L.W., DeMiguel, D., Robles, J.M., Furió, M., Van Dam, J., Garcés, M., Angelone, C., Moyà-Solà, S., 2016a. The Miocene mammal record of the Vallès-Penedès Basin (Catalonia). *C. R. Palevol.* 15, 791–812.
- Casanovas-Vilar, I., Garcés, M., Van Dam, J., García-Paredes, I., Robles, J.M., Alba, D.M., 2016b. An updated biostratigraphy for the late Aragonian and Vallesian of the Vallès-Penedès Basin (Catalonia). *Geol. Acta* 14, 195–217.
- Casanovas-Vilar, I., Torres, J., DeMiguel, D., Alba, D.M., 2018. Introducing: The Vallès-Penedès Miocene vertebrates paleobiodiversity database. In: *The Role of NOW in the Future of the Past*. NOW meeting in Bratislava 9–10 October 2018. Abstract book, pp. 1–2.
- Casanovas-Vilar, I., Kimura, Y., Flynn, L.J., Pilbeam, D., Moyà-Solà, S., Alba, D.M., 2019. Stable isotopes of rodent tooth enamel provide new evidence on Miocene ape environments in the Vallès-Penedès Basin (Catalonia). In: *The Palaeontological Association 63rd Annual Meeting*. 15th–21st December 2019. Programme Abstracts AGM Papers. University of Valencia, Spain, p. 28.
- Casanovas-Vilar, I., Kimura, Y., Flynn, L.J., Pilbeam, D., Moyà-Solà, S., Alba, D.M., 2020. Rodent stable isotopes provide new data on Miocene ape environments in the Siwaliks and the Vallès-Penedès Basin. *Am. J. Phys. Anthropol.* 171 (S69), 46.
- Chessel, D., Dufour, A., Thioulouse, J., 2004. The ade4 package – I: One-table methods. *R News* 4, 5–10.
- Collyer, M.L., Adams, D.C., 2018. RRRP: An R package for fitting linear models to high-dimensional data using residual randomization. *Methods Ecol. Evol.* 9, 1772–1779.
- Collyer, M.L., Adams, D.C., 2019. RRRP: Linear model evaluation with randomized residuals in a permutation procedure. R package version 1.3.1. <https://CRAN.R-project.org/package=RRRP>.
- Costeur, L., 2005. Cenogram analysis of the Rudabánya mammalian community: Palaeoenvironmental interpretations. *Paleontogr. Ital.* 90, 303–307.
- Crusafont Pairó, M., 1952. Los jiráfidos fósiles de España. *Mem. Comun. Inst. Geol.* 8, 1–239.
- Crusafont Pairó, M., 1958. Nuevo hallazgo del póngido vallesense *Hispanopithecus*. *Bol. Inf. A.E.P.V.* 1, 13–14.
- Crusafont Pairó, M., 1965. El desarrollo de los caninos en algunos Driopitécidos del Vallesense en Cataluña. *Not. Com. Inst. Geol. Min. Esp.* 80, 179–191.
- Crusafont Pairó, M., 1969. *Història de la paleontologia a Sabadell*. Joan Sallent Sucre, Sabadell.
- Crusafont Pairó, M., Villalta Comella, J.F. de, 1948. El Mioceno continental del Vallés y sus yacimientos de Vertebrados. *Publ. Fund. Bosch Cardellach* 3, 7–30.
- Crusafont Pairó, M., Hürzeler, J., 1961. Les Pongidés fossiles d'Espagne. *C. R. Acad. Sci. Paris* 252, 582–584.
- Crusafont Pairó, M., Hürzeler, J., 1969. Catálogo comentado de los Póngidos fósiles de España. *Acta Geol. Hisp.* 4, 44–48.
- Crusafont Pairó, M., Golpe Posse, J.M., 1973. New pongids from the Miocene of Vallès Penedès Basin (Catalonia, Spain). *J. Hum. Evol.* 2, 17–24.
- Crusafont Pairó, M., Gibert Cols, J., 1974. Nuevos datos sobre el género *Postpalerinaceus* del Vallesense. *Acta Geol. Hisp.* 9, 1–3.
- de Bonis, L., Abella, J., Merceron, G., Begun, D.R., 2017. A new late Miocene ailuropodine (giant panda) from Rudabánya (Northcentral Hungary). *Geobios* 50, 413–421.
- De Bruijn, H., Daams, R., Daxner-Höck, G., Fahlbusch, V., Ginsburg, L., Mein, P., Morales, J., 1992. Report of the RCMNS working group on fossil mammals, Reinsburg 1990. *Newsl. Stratigr.* 26, 65–118.
- DeMiguel, D., Alba, D.M., Moyà-Solà, S., 2014. Dietary specialization during the evolution of Western Eurasian hominoids and the extinction of European great apes. *PLoS One* 9, e97442.
- Domingo, L., Koch, P.L., Hernández Fernández, M., Fox, D.L., Domingo, M.S., Alberdi, M.T., 2013. Late Neogene and early Quaternary paleoenvironmental and paleoclimatic conditions in southwestern Europe: Isotopic analyses on mammalian taxa. *PLoS One* 8, e63739.
- Dray, S., Dufour, A., 2007. The ade4 package: Implementing the duality diagram for ecologists. *J. Stat. Softw.* 22, 1–20.
- Dray, S., Dufour, A., Chessel, D., 2007. The ade4 package – II: Two-table and K-table methods. *R News* 7, 47–52.
- Eastham, L., Skinner, M., Begun, D.R., 2009. Resolving seasonal stress in the Late Miocene hominoid *Hispanopithecus laietanus* through the analysis of the dental developmental defect linear enamel hypoplasia. *J. Vert. Paleontol.* 29, 91A.
- Eastham, L.C., Feranec, R.S., Begun, D.R., 2016. Stable isotopes show resource partitioning among the early Late Miocene herbivore community at Rudabánya II: Palaeoenvironmental implications for the hominoid, *Rudapithecus hungaricus*. *Paleoecogr. Palaeoclimatol. Palaeoecol.* 454, 161–174.
- Eastham, L.C., Feranec, R.S., Begun, D.R., 2017. Trace element analysis provides insight into the diets of early Late Miocene ungulates from the Rudabánya II locality (Hungary). *Geol. Acta* 15, 231–243.
- Eronen, J.T., Atabadi, M.M., Micheels, A., Karne, A., Bernor, R.L., Fortelius, M., 2009. Distribution history and climatic controls of Late Miocene Pikermian chronofauna. *Proc. Natl. Acad. Sci. USA* 106, 11867–11871.

- Eronen, J.T., Puolamäki, K., Liu, L., Lintulaakso, K., Damuth, J., Janis, C., Fortelius, M., 2010a. Precipitation and large herbivorous mammals II: Application to fossil data. *Evol. Ecol. Res.* 12, 235–248.
- Eronen, J., Polly, P., Fred, M., Damuth, J., Frank, D., Mosbrugger, V., Scheidegger, C., Stenseth, N., Fortelius, M., 2010b. Ecometrics: The traits that bind the past and present together. *Integr. Zool.* 5, 88–101.
- Eronen, J.T., Puolamäki, K., Liu, L., Lintulaakso, K., Damuth, J., Janis, C., Fortelius, M., 2010c. Precipitation and large herbivorous mammals I: Estimates from present-day communities. *Evol. Ecol. Res.* 12, 217–233.
- Fortelius, M., Van der Made, J., Bernor, R.L., 1996a. Middle and Late Miocene Suidae of Central Europe and the Eastern Mediterranean: Evolution, biogeography, and paleoecology. In: Bernor, R.L., Fahlbusch, V., Mittmann, H.W. (Eds.), *The Evolution of Western Eurasian Neogene Faunas*. Columbia University Press, New York, pp. 348–377.
- Fortelius, M., Werdelin, L., Andrews, P., Bernor, R.L., Gentry, A., Humphrey, L., Mittmann, H.-W., Viratana, S., 1996b. Provinciality, diversity, turnover, and paleoecology in land mammal faunas of the Later Miocene of Western Eurasia. In: Bernor, R.L., Fahlbusch, V., Mittmann, H.W. (Eds.), *The Evolution of Western Eurasian Neogene Faunas*. Columbia University Press, New York, pp. 414–448.
- Fortelius, M., Eronen, J.T., Jernvall, J., Liu, L., Pushkina, D., Rinne, J., Tesakov, A., Vislobokova, I., Zhang, Z., Zhou, L., 2002. Fossil mammals resolve regional patterns of Eurasian climate change during 20 million years. *Evol. Ecol. Res.* 4, 1005–1016.
- Fortelius, M., Zliobaitė, I., Kaya, F., Bibi, F., Bobe, R., Leakey, L., Leakey, M., Patterson, D., Rannikko, J., Werdelin, L., 2016. An ecometric analysis of the fossil mammal record of the Turkana Basin. *Philos. Trans. R. Soc. B* 371, 20150232.
- Furió, M., Prieto, J., Van den Hoek Ostende, L., 2015. Three million years of “Terror-Shrew” (*Dinosorex*, Eulipotyphla, Mammalia) in the Miocene of the Vallès-Penedès Basin (Barcelona, Spain). *C. R. Palevol.* 14, 111–124.
- Galbrun, E., Tang, H., Fortelius, M., Zliobaitė, I., 2018. Computational biomes: The ecometrics of large mammal teeth. *Paleontol. Electron.* 21, 21.1.3A.
- Garcés, M., Agustí, J., Cabrera, L., Parés, J.M., 1996. Magnetostratigraphy of the Vallesian (late Miocene) in the Vallès-Penedès Basin (northeast Spain). *Earth Plant. Sci. Lett.* 142, 381–396.
- Golpe-Posse, J.M., 1971. *Suiformes del Terciario español y sus yacimientos*. Ph.D. Dissertation, Universidad de Barcelona.
- Golpe-Posse, J.M., 1972. *Suiformes del terciario español y sus yacimientos* (Tesis doctoral-Resumen) (revisado y reimprimido en Diciembre de 1972). *Paleontol. Evol.* 2, 1–197.
- Golpe Posse, J.M., 1982. Los hispanopitecos (Primates, Pongidae) de los yacimientos del Vallès Penedès (Cataluña – España). I: Material ya descrito. *Bull. Inf. Inst. Paleontol. Sabadell* 14, 63–69.
- Golpe Posse, J.M., 1993. Los Hispanopitecos (Primates, Pongidae) de los yacimientos del Vallès-Penedès (Cataluña, España). II: Descripción del material existente en el Instituto de Paleontología de Sabadell. *Paleontol. Evol.* 26–27, 151–224.
- Golpe-Posse, J.M., Crusafont Pairó, M., 1982. Caracterización de *Tapirus priscus* Kaup en el Mioceno superior del Vallès-Penedès. *Acta Geol. Hisp.* 17, 95–101.
- Harrison, T., 1991. Some observations on the Miocene hominoids from Spain. *J. Hum. Evol.* 20, 515–520.
- Heissig, K., 1999. Family Chalicotheriidae. In: Rössner, G.E., Heissig, K. (Eds.), *The Miocene Land Mammals of Europe*. Verlag Dr. Friedrich Pfeil, München, pp. 189–192.
- Hernández Fernández, M., Salesa, M.J., Sánchez, I.M., Morales, J., 2003. Paleocología del género *Anchitherium* von Meyer, 1834 (Equidae, Perissodactyla, Mammalia) en España: Evidencias a partir de las faunas de macromamíferos. *Col. Paleontol.* 1, 253–280.
- Higgins, P., 2018. Isotope ecology from biominerals. In: Croft, D.A., Su, D.F., Simpson, S. W. (Eds.), *Methods in Paleoecology*. Springer, Cham, pp. 99–120.
- Hilgen, F.J., Lourens, L.J., Van Dam, J.A., 2012. The Neogene period. In: Gradstein, F.M., Ogg, J.G., Schmitz, M., Ogg, G. (Eds.), *The Geologic Time Scale 2012*. Elsevier, Amsterdam, pp. 923–978.
- Hunter, J.P., Fortelius, M., 1994. Comparative dental occlusal morphology, facet development, and microwear in two sympatric species of *Listriodon* (Mammalia: Suidae) from the Middle Miocene of Western Anatolia (Turkey). *J. Vertebr. Paleontol.* 14, 105–126.
- Iannucci, A., Begun, D.R., 2022. Suidae (Mammalia, Artiodactyla) from the late Miocene hominoid locality of Alsótelekes (Hungary). *Geobios* 71, 39–49.
- Jackson, S., 2012. *Gliding Mammals of the World*. CSIRO Publishing, Collingwood.
- Jernvall, J., 1995. Mammalian molar cusp patterns: Developmental mechanisms of diversity. *Acta Zool. Fenn.* 198, 1–61.
- Kassambara, A., Mundt, F., 2020. factextra: Extract and visualize the results of multivariate data analyses. R package version 1.0.7. <https://CRAN.R-project.org/package=factextra/>.
- Kaya, F., Bibi, F., Zliobaitė, I., Eronen, J.T., Hui, T., Fortelius, M., 2018. The rise and fall of the Old World savannah fauna and the origins of the African savannah biome. *Nat. Ecol. Evol.* 2, 241–246.
- Koch, P.L., 1998. Isotopic reconstruction of past continental environments. *Ann. Rev. Earth Plant. Sci.* 26, 573–613.
- Kohn, M.J., 2010. Carbon isotope compositions of terrestrial C3 plants as indicators of (paleo)ecology and (paleo)climate. *Proc. Natl. Acad. Sci. USA* 107, 19691–19695.
- Kohn, M.J., Schoeninger, M.J., Valley, J.W., 1998. Variability in oxygen isotope compositions of herbivore teeth: Reflections of seasonality or developmental physiology? *Chem. Geol.* 152, 97–112.
- Köhler, M., 1993. Skeleton and habitat of recent and fossil ruminants. *Münch. Geowiss. Abh. A* 25, 1–88.
- Liu, L., Puolamäki, K., Eronen, J., Ataabadi, M.M., Hernesniemi, E., Fortelius, M., 2012. Dental functional traits of mammals resolve productivity in terrestrial ecosystems past and present. *Proc. R. Soc. B* 279, 2793–2799.
- Lu, X., Ge, D., Xia, L., Zhang, Z., Li, S., Yang, Q., 2013. The evolution and paleobiogeography of flying squirrels (Sciuridae, Pteromyini) in response to global environmental change. *Evol. Biol.* 40, 117–132.
- Marmi, J., Casanovas-Vilar, I., Robles, J.M., Moyà-Solà, S., Alba, D.M., 2012. The paleoenvironment of *Hispanopithecus laietanus* as revealed by paleobotanical evidence from the Late Miocene of Can Llobateres 1 (Catalonia, Spain). *J. Hum. Evol.* 62, 412–423.
- Mazo, A.V., 1977. *Revisión de los mastodontes de España*. Ph.D. Dissertation, Universidad Complutense de Madrid.
- Mazo, A.V., Van der Made, J., 2012. Iberian mastodonts: Geographic and stratigraphic distribution. *Quat. Int.* 255, 239–256.
- McKenzie, S., Sorbelli, L., Cherin, M., Almécija, S., Pina, M., Abella, J., Luján, A.H., DeMiguel, D., Alba, D.M., 2023. Earliest Vallesian suid remains from Creu de Conill 20 (Vallès-Penedès Basin, NE Iberian Peninsula). *J. Mamm. Evol.* 30, 155–212.
- Mein, P., 1990. Updating of MN zones. In: Lindsay, E.H., Fahlbusch, V., Mein, P. (Eds.), *European Neogene Mammal Chronology*. Springer, Boston, pp. 73–90.
- Merceron, G., Kaiser, T.M., Kostopoulos, D.S., Schulz, E., 2010. Ruminant diets and the Miocene extinction of European great apes. *Proc. R. Soc. B* 277, 3105–3112.
- Misas Alcántara, M., 2022. El paleoambiente d’*Hispanopithecus laietanus*: noves dades basades en l’anàlisi d’isòtops estables de l’esmal dental dels mamífers herbívors de Can Llobateres. B.Sc. Thesis, Universitat Autònoma de Barcelona.
- Moyà-Solà, S., 1979. *Revisión del género Dorcatherium* Kaup, 1833 (Mammalia, Ruminantia, Tragulidae) de las cuencas miocénicas catalanas. *Bull. Inf. Inst. Paleontol. Sabadell* 11, 55–59.
- Moyà-Solà, S., 1983. Los Boselaphini (Bovidae Mammalia) del Neógeno de la Península Ibérica. Universidad Autónoma de Barcelona, Barcelona.
- Moyà-Solà, S., Agustí, J., 1990. Bioevents and mammal successions in the Spanish Miocene. In: Lindsay, E.H., Fahlbusch, V., Mein, P. (Eds.), *European Neogene Mammal Chronology*. Plenum Press, New York, pp. 357–373.
- Moyà-Solà, S., Köhler, M., 1993. Recent discoveries of *Dryopithecus* shed new light on evolution of great apes. *Nature* 365, 543–545.
- Moyà-Solà, S., Köhler, M., 1995. New partial cranium of *Dryopithecus* Lartet, 1863 (Hominoidea, Primates) from the upper Miocene of Can Llobateres, Barcelona, Spain. *J. Hum. Evol.* 29, 101–139.
- Moyà-Solà, S., Köhler, M., 1996. A *Dryopithecus* skeleton and the origins of great-ape locomotion. *Nature* 379, 156–159.
- Moyà-Solà, S., Pons-Moyà, J., Köhler, M., 1990. Primates catarrinos (Mammalia) del Neógeno de la península Ibérica. *Paleontol. Evol.* 23, 41–45.
- Moyà-Solà, S., Köhler, M., Alba, D.M., Casanovas-Vilar, I., Galindo, J., Robles, J.M., Cabrera, L., Garcés, M., Almécija, S., Beamud, E., 2009. First partial face and upper dentition of the Middle Miocene hominoid *Dryopithecus fontani* from Abocador de Can Mata (Vallès-Penedès Basin, Catalonia, NE Spain): Taxonomic and phylogenetic implications. *Am. J. Phys. Anthropol.* 139, 126–145.
- Nagatoshi, K., 1987. Miocene hominoid environments of Europe and Turkey. *Palaeogeogr. Palaeoclimatol. Palaeoecol.* 61, 145–154.
- Oksanen, O., Zliobaitė, I., Saarinen, J., Lawing, A.M., Fortelius, M., 2019. A Humboldtian approach to life and climate of the geological past: Estimating palaeotemperature from dental traits of mammalian communities. *J. Biogeogr.* 46, 1760–1776.
- Peel, M.C., Finlayson, B.L., McMahon, T.A., 2007. Updated world map of the Köppen-Geiger climate classification. *Hydro. Earth Syst. Sci.* 11, 1633–1644.
- Pickford, M., 1981. *Parachleuastocherus* (Mammalia, Suidae). *Estud. Geol.* 37, 313–320.
- Pickford, M., 2014. *Sus valentini* Filhol (1882) from St Gaudens (MN 8–9) France: Blighted from the outset but a key to understanding late Middle Miocene Tetraconodontinae (Suidae, Mammalia) of Europe. *Mainz. Naturwiss. Arch.* 51, 167–220.
- Pickford, M., 2016. Biochronology of European Miocene Tetraconodontinae (Suidae, Artiodactyla, Mammalia) flowing from recent revision of the subfamily. *Ann. Naturhist. Mus. Wien* 118, 175–244.
- Pickford, M., Pourabrisshami, Z., 2013. Deciphering Dinotheriensande deinotheriid diversity. *Palaeobiodiv. Palaeoenviron.* 93, 121–150.
- Pickford, M., Moyà Solà, S., Mein, P., 1997. A revised phylogeny of Hyracoidea (Mammalia) based on new specimens of Pliohyracidae from Africa and Europe. *Neues Jahrb. Geol. Paläont. Abh.* 205, 265–288.
- Pina, M., Alba, D.M., Almécija, S., Fortuny, J., Moyà-Solà, S., 2012. Brief communication: Paleobiological inferences on the locomotor repertoire of extinct hominoids based on femoral neck cortical thickness: The fossil great ape *Hispanopithecus laietanus* as a test-case study. *Am. J. Phys. Anthropol.* 149, 142–148.
- Pugh, K.D., 2022. Phylogenetic analysis of Middle-Late Miocene apes. *J. Hum. Evol.* 165, 103140.
- R Core Team, 2021. *R: A language and environment for statistical computing*. R Foundation for Statistical Computing, Vienna. <https://www.R-project.org/>.
- Ribot, F., Gibert, J., Harrison, T., 1996. A reinterpretation of the taxonomy of *Dryopithecus* from Vallès-Penedès, Catalonia (Spain). *J. Hum. Evol.* 31, 129–141.
- Robles, J.M., Abella, J., Madurell-Malapeira, J., Alba, D.M., 2014. Miocene carnivorans from the Vallès-Penedès Basin. In: Robles, J.M. (Ed.), *Miocene carnivorans from the Vallès-Penedès Basin (NE Iberian Peninsula)*. Ph.D. Dissertation, Universitat Autònoma de Barcelona, pp. 367–434.
- RStudio Team, 2021. *RStudio: Integrated Development Environment for R*. RStudio, PBC, Boston. <http://www.rstudio.com/>.
- Sanisidro, O., Cantalapietra, J.L., 2022. The Rhinocerotidae fossil record in the Iberian Peninsula. *Hist. Biol.* 34, 1591–1610.
- Santafé Llopis, J.V., 1978. *Rinocerótidos fósiles de España*. Ph.D. Dissertation, Universidad de Barcelona.

- Sanz de Siria Catalán, A., 1993. Datos sobre la paleoclimatología y paleoecología del Neógeno del Vallès-Penedès según las macrofloras halladas en la Cuenca y zonas próximas. *Paleontol. Evol.* 26–27, 281–289.
- Sanz de Siria Catalán, A., 1994. La evolución de las paleofloras en las cuencas cenozoicas catalanas. *Acta Geol. Hisp.* 29, 169–189.
- Schlager, S., 2017. Morpho and Rvcg – Shape analysis in R. In: Zheng, G., Li, S., Székely, G. (Eds.), *Statistical Shape and Deformation Analysis*. Academic Press, London, pp. 217–256.
- Sinita, M.V., Cermák, S., Kryuchkova, L.Y., 2022. Cranial anatomy of *Csakvaromys bredai* (Rodentia, Sciuridae, Xerinae) and Implications for ground squirrel evolution and systematics. *J. Mamm. Evol.* 29, 149–189.
- Skinner, M.F., Dupras, T.L., Moyà-Solà, S., 1995. Periodicity of linear enamel hypoplasia among Miocene *Dryopithecus* from Spain. *J. Paleopathol.* 7, 195–222.
- Stefan, V., Levin, S., 2022. plotbiomes: Plot Whittaker biomes with ggplot2. R package version 0.0.0.9001. <https://rdrr.io/github/valentininrelav/plotbiomes/>.
- Susanna, I., Alba, D.M., Almécija, S., Moyà-Solà, S., 2014. The vertebral remains of the late Miocene great ape *Hispanopithecus laietanus* from Can Llobateres 2 (Vallès-Penedès Basin, NE Iberian Peninsula). *J. Hum. Evol.* 73, 15–34.
- Szalay, F., Delson, E., 1979. *Evolutionary History of the Primates*. Academic Press, New York.
- Tallman, M., Almécija, S., Reber, S.L., Alba, D.M., Moyà-Solà, S., 2013. The distal tibia of *Hispanopithecus laietanus*: More evidence for mosaic evolution in Miocene apes. *J. Hum. Evol.* 62, 319–327.
- The NOW Community, 2023. *New and Old Worlds Database of Fossil Mammals (NOW)* Licensed under CC BY 4.0. <https://nowdatabase.org/now/database/>, 2023. (Accessed 31 May 2023).
- Thioulouse, J., Dray, S., Dufour, A., Siberchicot, A., Jombart, T., Pavoine, S., 2018. *Multivariate Analysis of Ecological Data with ade4*. Springer, New York.
- Toivonen, J., Fortelius, M., Žliobaitė, I., 2022. Do species factories exist? Detecting exceptional patterns of evolution in the mammalian fossil record. *Proc. R. Soc. B* 289, 20212294.
- Ungar, P.S., 1996. Dental microwear of European Miocene catarrhines: Evidence for diets and tooth use. *J. Hum. Evol.* 31, 335–366.
- Urciuoli, A., Alba, D.M., 2023. Systematics of Miocene apes: State of the art of a never-ending controversy. *J. Hum. Evol.* 175, 103309.
- Valenciano, A., Jiangzuo, Q., Wang, S., Li, C., Zhang, X., Ye, J., 2019. First record of *Hoplictis* (Carnivora, Mustelidae) in East Asia from the Miocene of the Ulungur River Area, Xianjiang, Northwest China. *Acta Geol. Sin.* 93, 251–264.
- Van Dam, J.A., Krijgsman, W., Abels, H.A., Álvarez-Sierra, M.Á., García-Paredes, I., López-Guerrero, P., Peláez-Campomanes, P., Venter, D., 2014. Updated chronology for Middle to Late Miocene mammal sites of the Daroca área (Calatayud-Montalbán Basin, Spain). *Geobios* 47, 325–334.
- Van den Hoek Ostende, L.W., Furió, M., 2005. Spain. In: van den Hoek Ostende L.W., Doukas C.S., Reumer J.W.F. (Eds.), *The Fossil Record of the Eurasian Neogene Insectivores (Erinaceomorpha, Soricomorpha, Mammalia)*, Part I. *Scripta Geol. Special Issue* 5, 149–284.
- Van der Made, J., 1990. Iberian Suoidea. *Paleontol. Evol.* 23, 83–97.
- Van der Made, J., 1996. *Listriodontinae* (Suidae, Mammalia), their evolution, systematics and distribution in time and space. *Contrib. Tert. Quat. Geol.* 33, 3–254.
- Van der Made, J., 1997. Los Suoidea de la Península Ibérica. In: Calvo, J.P., Morales, J. (Eds.), *Avances en el conocimiento del Terciario Ibérico*. Cuenca, pp. 109–112.
- Van der Made, J., 2010. The pigs and “Old World peccaries” (Suidae and Palaeochoeridae, Suoidea, Artiodactyla) from the Miocene of Sandelzhausen (southern Germany): Phylogeny and an updated classification of the Hyotheriinae and Palaeochoeridae. *Paläontol. Zeits.* 84, 43–121.
- Van der Made, J., Krakhmalnaya, T., Kubiak, H., 1999. The pig *Propotamochoerus palaeochoerus* from the upper Miocene of Grytsiv, Ukraine. *Estud. Geol.* 55, 283–292.
- Van der Made, J., Aiglstorfer, M., Böhme, M., 2014. Taxonomic study of the pigs (Suidae, Mammalia) from the late Middle Miocene of Gratkorn (Austria, Syria). *Palaeobiodiv. Palaeoenviro.* 94, 595–617.
- Van der Made, J., Choudhary, D., Singh, N.P., Sharma, K.M., Singh, N.A., Patnaik, R., 2022. *Listriodon dukkar* sp. nov. (Suidae, Artiodactyla, Mammalia) from the late Miocene of Pasuda (Gujarat, India): The decline and extinction of the Listriodontinae. *Paläontol. Zeits.* 96, 355–383.
- Vermillion, W., Polly, P., Head, J., Eronen, J., Lawing, A., 2018. Ecometrics: A trait-based approach to paleoclimate and paleoenvironmental reconstruction. In: Croft, D.A., Su, D.F., Simpson, S.W. (Eds.), *Methods in Paleocology. Reconstructing Cenozoic Terrestrial Environments and Ecological Communities*. Springer Nature Switzerland, Cham, pp. 373–394.
- Villalta Comella, J.F. de, Crusafont Pairó, M., 1943. Los Vertebrados del Mioceno continental de la cuenca del Vallès-Penedés (provincia de Barcelona): I. Insectívoros; II. Carnívoros. *Bol. Inst. Geol. Min. Esp.* 56, 147–314.
- Walter, H., 1979. *Vegetation und Klimazonen*, 4th ed. Verlag Eugen Ulmer, Stuttgart.
- Wickham, H., 2016. *ggplot2: Elegant Graphics for Data Analysis*. Springer-Verlag, New York. <https://ggplot2.tidyverse.org/>.
- Wickham, H., Hester, J., Chang, W., Bryan, J., 2021. devtools: Tools to make developing R packages easier. R package version 2.4.3. <https://CRAN.R-project.org/package=devtools/>.
- Whittaker, R., 1975. *Communities and Ecosystems*, 2nd ed. MacMillan Publishing Co., New York.
- Zanoli, C., Bouchet, F., Fortuny, J., Bernardini, F., Tuniz, C., Alba, D.M., 2023. A reassessment of the distinctiveness of dryopithecine genera from the Iberian Miocene based on enamel-dentine junction geometric morphometric analyses. *J. Hum. Evol.* 177, 103326.
- Žliobaitė, I., Rinne, J., Tóth, A., Mechenich, M., Liu, L., Behrensmeier, A., Fortelius, M., 2016. Herbivore teeth predict climatic limits in Kenyan ecosystems. *Proc. Natl. Acad. Sci. USA* 113, 12751–12756.
- Žliobaitė, I., Tang, H., Saarinen, J., Fortelius, M., Rinne, J., Rannikko, J., 2018. Dental ecometrics of tropical Africa: Linking vegetation types and communities of large plant-eating mammals. *Evol. Ecol. Res.* 19, 127–147.